Equilibria, Stability, and Transients in Re-entrant Lines under FBFS and LBFS Dispatch and Constant Release

Michael Hassoun[a], Semyon M. Meerkov[a], and Chao-Bo Yan[a,b]

[a] Department of Electrical Engineering and Computer Science
University of Michigan, Ann Arbor, MI 48109-2122
[b] Center for Intelligent and Networked Systems (CFINS)
Department of Automation and TNList
Tsinghua University, Beijing 100084, China

Abstract

A model of a re-entrant line, consisting of the bottleneck workcenter and time delays representing other workcenters, is considered. Its mathematical description is provided and performance metrics are introduced. The steady states of this model and their stability properties are investigated under two dispatch policies – First Buffer First Served (FBFS) and Last Buffer First Served (LBFS) – and under constant release rate. The transients due to machine downtime are also analyzed. It is shown that, although LBFS may be viewed as having superior steady state characteristics, it induces longer and more volatile transients than FBFS and, in some cases, periodic and chaotic regimes.

Keywords: Re-entrant lines, FBFS and LBFS dispatch, nonlinear dynamics, steady states, finite-time stability, transients, throughput variability, periodic and chaotic regimes.

1 Introduction

Equilibria, stability, and transients in serial production lines and assembly systems have been investigated analytically for over 50 years (see, for instance, monographs [1]-[5]). For re-entrant lines these issues have been analyzed to a much lesser extent. The purpose of this paper is to contribute to this end.

To simplify the analysis, we make the following assumptions:

A.1 The system has a bottleneck workcenter (BNWC) and, thus, the approach proposed by O. Rose [6]-[9] can be used. According to this approach, only the BNWC, i.e., the workcenter with the largest utilization, is modeled in details, while all other workcenters and queueing therein are viewed as time delays. A slightly modified version of Rose's model is shown in Figure 1.1, where m_i, $i = 1, 2, \dots, M$, are the BNWC machines (tools); b_i, $i = 1, 2, \dots, N$, are the BNWC buffers storing parts (lots) at various stages of their processing; p_i, $i = 1, 2, \dots, N-1$, are the re-entrant paths modeled as time delays; and p_0 and p_N are the input and output paths, respectively, also modeled as time delays.

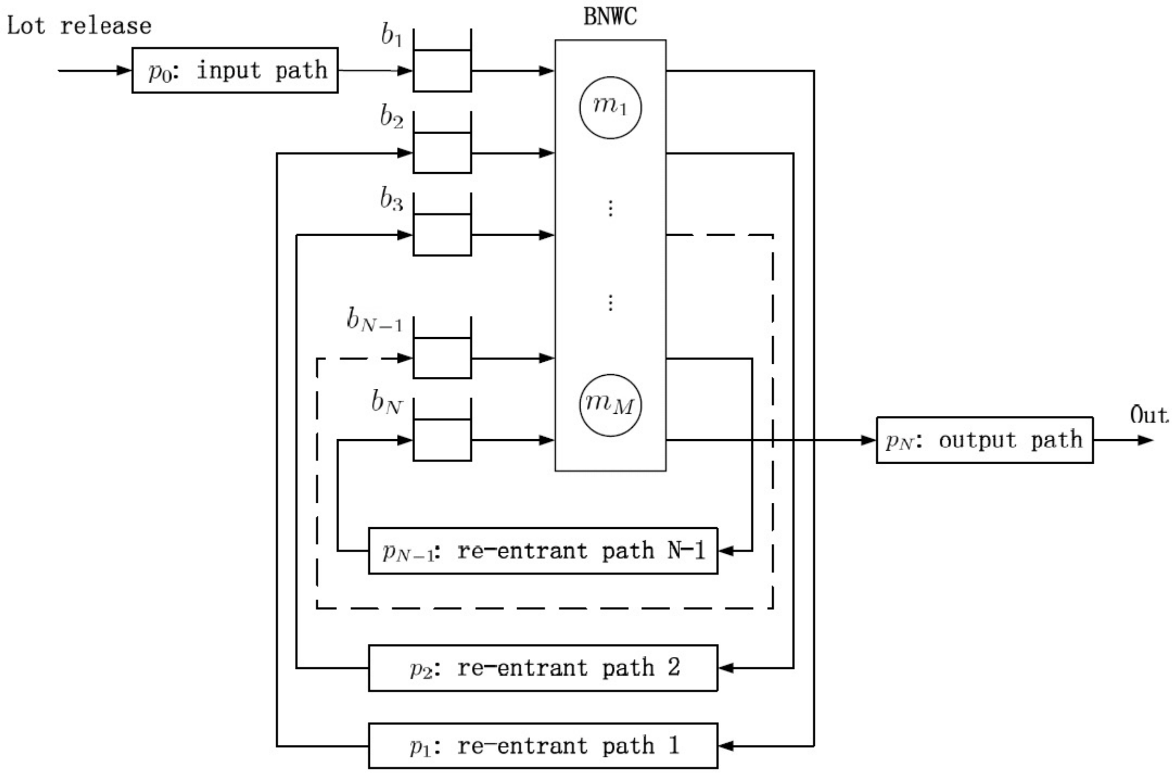

Figure 1.1: BNWC-based model of re-entrant line

A.2 All buffers are of infinite capacity and, thus, no blockage takes place.

A.3 The machines of the BNWC may go down (due to either breakdown or preventive maintenance) and remain down for a certain period of time.

Under these assumptions, we study static and dynamic properties of re-entrant lines with two dispatch policies – First Buffer First Served (FBFS) and Last Buffer First Served (LBFS) – and a constant release rate. Other dispatch and release policies can be analyzed similarly. According to FBFS, the BNWC machines are first assigned to process lots from buffer b_1; the remaining machines, if any, are allocated to buffer b_2, and so on until either the machines or the lots are exhausted. In LBFS, the priority is reversed, i.e., the machines are first assigned to process lots from buffer b_N, then from b_{N-1}, and so on. Note that under any dispatch policy, the re-entrant line of Figure 1.1 can be represented as a serial line shown in Figure 1.2, where the number of machines, allocated for processing lots from buffer b_i, $i = 1, 2, \ldots, N$, depends on the dispatch policy and buffer occupancies. Note also that if the machines were allocated in a fixed manner (i.e., independent of the buffer priority and occupancy), a re-entrant line would become the usual serial line with a fixed number of machines in each operation.

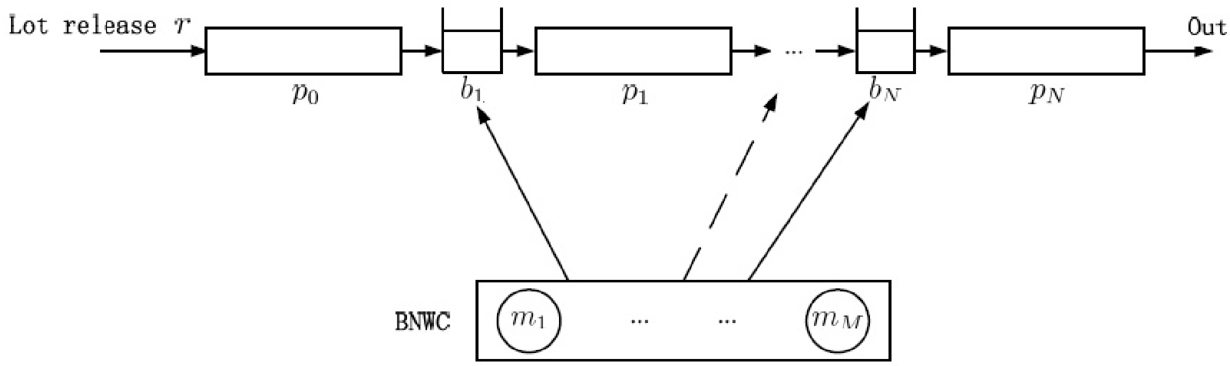

Figure 1.2: Equivalent representation of the BNWC-based model of re-entrant line

The main results of this study are as follows:

- **Steady States**: Under-loaded systems (i.e., systems with the release rate smaller than the BNWC capacity) have a unique steady state for both FBFS and LBFS dispatch. Fully-loaded systems (release rate equals the BNWC capacity) have multiple equilibria; for FBFS these equilibria are characterized by excessive inventory in the last buffer; for LBFS they have excessive inventory in the first buffer. Over-loaded systems have no steady states.

- **Stability**: Under FBFS, the unique steady state is finite-time stable and globally attractive (i.e., the system reaches its equilibrium in finite time from any non-negative bounded initial condition); it is finite-time stable but not globally attractive under LBFS (unless the delays in all re-entrant paths are identical). The multiple equilibria are not globally attractive for both FBFS and LBFS dispatch.

- **Transients**: Under LBFS, the transients due to machine downtime may be an order of magnitude longer and up to three orders of magnitude more variable than those under FBFS, although LBFS leads to a somewhat smaller excess of work-in-process and residence time (system cycle time).

Based on the above, the main insight provided by this study is as follows: In systems where machine downtimes are common and the release is constant, LBFS (and other disciplines favoring almost completed lots) should be avoided, if the duration of transients and the variability of throughput and work-in-process are of concern.

The work reported here has been inspired by the research initiated in [10] and [6]. In [10], along with investigating chaotic regimes, the authors posed several questions related to the re-entrant line steady states (or, more generally, attractors) and their stability properties. Some of the answers have been provided in [11], but the effects of dispatch policies have not been analyzed. In [6], the issues of transients due to catastrophic failures of BNWC have been investigated by simulations, but no analytical results have been presented. In addition, our work benefited from the research of [12] on stability of scheduling policies and of [13] and [14] on steady state performance of re-entrant lines.

It should be pointed out that majority of the results reported in the literature on analysis of re-entrant lines are obtained by simulations (e.g., [6]-[10], [13]-[18]). Some analytical results are also available. Along with [11] and [12], these include [19]-[21], where a fluid model approach is applied to stability analysis of re-entrant lines, and [22]-[24], where the issues of performance analysis are investigated using both queueing theory and recursive aggregation techniques. In our work, analytical and numerical approaches are used. Within the analytical approach, we construct difference equations that describe systems at hand and study their properties, leading to various theorems. In the numerical approach, we solve these equations under appropriate initial conditions, leading to so-called numerical facts.

The outline of this paper is as follows: Section 2 addresses the issues of modeling and mathematical description of re-entrant lines at hand; also, various performance metrics are introduced, and the problems considered are formulated. The steady states of re-entrant lines and their stability properties are analyzed in Sections 3 and 4, respectively. Sections 5 and 6 are devoted to the transients induced by FBFS and LBFS, respectively, while Section 7 compares their properties. Section 8 presents several extensions. The conclusions and topics for future research are listed in Section 9. All proofs are given in the Appendix.

2 Modeling, Mathematical Description, and Problem Formulation

2.1 Model

We define the BNWC-based model of the re-entrant line by the following assumptions:

(i) The system consists of the BNWC with machines m_i, $i = 1, 2, \ldots, M$, buffers b_i, $i = 1, 2, \ldots, N$, re-entrant paths p_i, $i = 1, 2, \ldots, N-1$, input path p_0, and the output path p_N, arranged as shown in Figure 1.1.

(ii) Each machine m_i, $i = 1, 2, \ldots, M$, has the cycle time of duration η. The time axis is slotted with the slot duration η (a unit of time).

(iii) Each buffer b_i, $i = 1, 2, \ldots, N$, is of unlimited capacity.

(iv) Each re-entrant path p_i, $i = 1, 2, \ldots, N-1$, and the input and output paths p_0 and p_N, are delays of duration τ_i, $i = 0, 1, \ldots, N$ (in units of the machine cycle time).

(v) At each time slot $n = 1, 2, \ldots$, one or more machines may go down and remain down for T_{down} time slots.

(vi) The number of lots released at the beginning of each time slot is $r = const$.

(vii) The machines are assigned to process lots from buffer b_i, $i = 1, 2, \ldots, N$, according to a dispatch policy. A dispatch policy is closed-loop if the machine assignment depends on the buffer occupancies at the beginning of time slot n.

This model is considered throughout this paper for two closed-loop dispatch policies: FBFS and LBFS. Other dispatch policies and non-constant release rates can be analyzed in a similar manner.

Model (i)-(vii) can encompass large re-entrant lines by assuming $N \gg 1, \tau_i \gg 1, i = 1, 2, \ldots, N-1$, while τ_0 and τ_N may or may not be large. Also, model (i)-(vii) can be generalized to encompass machines with different cycle times and multi-product manufacturing. For the sake of simplicity, however, we limit our attention to the basic model and defer the generalizations to future work.

Clearly, model (i)-(vii) is a simplification of re-entrant lines with $K > 1$ workcenters (see Figure 2.1) under the assumption that the utilization of one of them (BNWC) is larger than of all the others. In this situation, the number of workcenters in each re-entrant path gives rise to the time delays, τ_i, involved in assumption (iv). Section 8 provides some quantitative results on accuracy of this simplification.

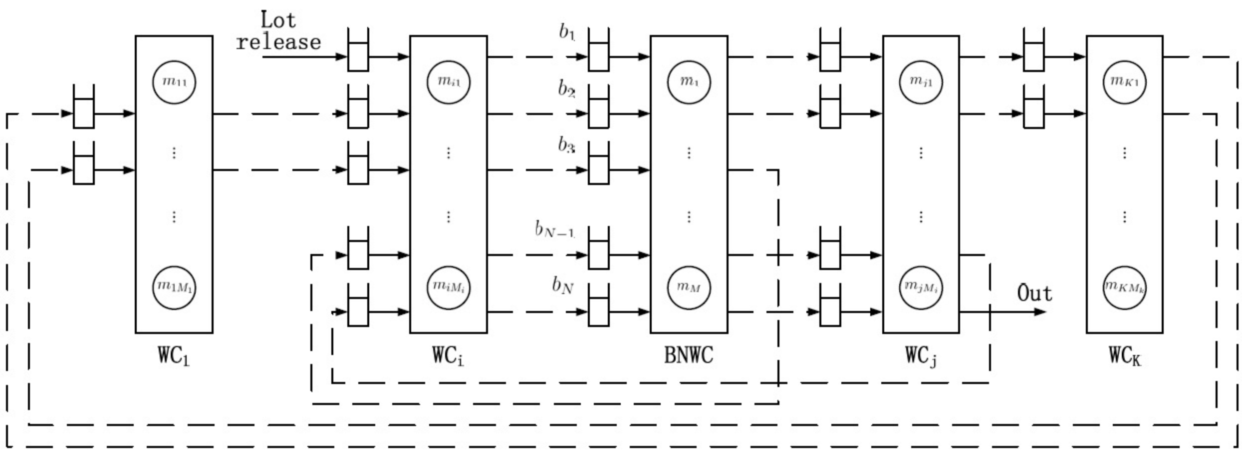

Figure 2.1: Re-entrant line with K workcenters

2.2 Mathematical description

2.2.1 General equations and performance metrics

Let $v_i(n)$ be the number of machines allocated (according to a certain dispatch policy) to buffer b_i at the beginning of time slot n. Then, the re-entrant line defined by assumptions (i)-(vii) can be described by the following *delay-difference* equations of dimensionality N:

$$\begin{aligned} x_1(n+1) =& x_1(n) + r - \min\{v_1(n), x_1(n)\}, \\ x_i(n+1) =& x_i(n) + \min\{v_{i-1}(n-\tau_{i-1}), x_{i-1}(n-\tau_{i-1})\} - \min\{v_i(n), x_i(n)\},\ i = 2, 3, \ldots, N, \end{aligned} \tag{2.1}$$

where $x_i(n)$ is the number of lots in buffer b_i at the beginning of slot n.

Let $z_{ij}(n)$, $i = 0, 1, \ldots, N$, $j = 1, 2, \ldots, \tau_i$, denote the number of lots in the delay path p_i processed j time slots prior to n. Then, in the extended form, the delay-difference equations (2.1) can be re-written as the following system of *difference* equations of dimensionality $N + \sum_{i=0}^{N} \tau_i$:

$$\begin{aligned} z_{01}(n+1) &= r, \\ z_{0j}(n+1) &= z_{0,j-1}(n), j = 2, 3, \ldots, \tau_0, \\ x_1(n+1) &= x_1(n) + z_{0,\tau_0}(n) - \min\{v_1(n), x_1(n)\}, \\ z_{i1}(n+1) &= \min\{v_i(n), x_i(n)\}, i = 1, 2, \ldots, N-1, \\ z_{ij}(n+1) &= z_{i,j-1}(n), i = 1, 2, \ldots, N-1, j = 2, 3, \ldots, \tau_i, \\ x_i(n+1) &= x_i(n) + z_{i-1,\tau_{i-1}}(n) - \min\{v_i(n), x_i(n)\}, i = 2, 3, \ldots, N, \\ z_{N1}(n+1) &= \min\{v_N(n), x_N(n)\}, \\ z_{Nj}(n+1) &= z_{N,j-1}(n), j = 2, 3, \ldots, \tau_N. \end{aligned} \tag{2.2}$$

Given (2.2), the *production rate*, $PR(n)$ (i.e., the number of lots that completed their processing during the n-th time slot) and the *work-in-process*, $WIP(n)$ (i.e., the number of lots in the system at the beginning of slot n) can be expressed as follows:

$$PR(n) = \begin{cases} \min\{v_N(n), x_N(n)\}, & \text{if } \tau_N = 0, \\ z_{N,\tau_N}(n), & \text{if } \tau_N \neq 0, \end{cases} \tag{2.3}$$

and

$$WIP(n) = \sum_{i=1}^{N} x_i(n) + \sum_{i=0}^{N} \sum_{j=1}^{\tau_i} z_{ij}(n). \tag{2.4}$$

We use the notion of the production rate, $PR(n)$, rather than the throughput, TP, since the latter, being the number of lots completed, for instance, per hour or per shift, is less suitable for transient performance analysis than the former.

Clearly, in the steady state,

$$PR(n) = PR_{ss},\ WIP(n) = WIP_{ss},\ RT_{ss} = \frac{WIP_{ss}}{PR_{ss}},$$

where RT_{ss} is *steady state residence time* (i.e., the time interval between a lot entering and leaving the system). Away from the steady state, we denote the residence time as $RT(n)$, which is the maximum residence time of the lots exiting the system at time slot n. As in the case of PR, we use the term residence time, rather than system cycle time or throughput time, because the latter are measures of the steady state operation, whereas our interest is in the dynamics as well.

Along with PR_{ss}, WIP_{ss}, and RT_{ss}, we consider the following metrics characterizing the transients. The first one is the *settling time*, T_s, defined as the time to return to the steady state after the machine(s) downtime of duration T_{down}:

$$T_s = T_s(T_{down}).$$

A related measure is the *relative settling time*, T_s^{rel}, which is T_s in units of T_{down}, i.e.,

$$T_s^{rel} = \frac{T_s}{T_{down}}. \tag{2.5}$$

The second transient performance measure is the *excess* of *WIP* defined as

$$EX_{WIP} = \frac{\sum_{n=n_0+1}^{n_0+T_{down}+T_s} WIP(n) - (T_{down}+T_s)WIP_{ss}}{(T_{down}+T_s)WIP_{ss}} \times 100\%, \tag{2.6}$$

where n_0 is the time slot when the machine(s) went down. Clearly, EX_{WIP} characterizes how much additional total *WIP* has been accumulated during the transient.

The third transient performance measure is the *overshoot of residence time*:

$$OS_{RT} = \frac{RT_{\max}(T_{down}) - RT_{ss}}{RT_{ss}} \times 100\%, \tag{2.7}$$

$$RT_{\max}(T_{down}) = \max_{k\in\{1,2,\ldots,(T_{down}+T_s)r\}} [n_{out}(k) - n_{in}(k) + 1],$$

where k denotes the k-th lot released during the breakdown and transient period, $T_{down} + T_s$, and $n_{in}(k)$ and $n_{out}(k)$ are the time slots when the k-th lot was released and completed its processing, respectively. Clearly, OS_{RT} quantifies how much the due date of a lot is exceeded if it were set based on RT_{ss}.

While the previous metrics address mostly $WIP(n)$, the next one is related to $PR(n)$. To introduce it, assume that *all* machines of the BNWC were down for T_{down} time slots and then went up and the system returned to the steady state after the settling time T_s. Let T_{zeroPR} denote the number of slots when no lots were produced at the output of the system during the interval $T_{down} + T_s$. Introduce the *relative zero-PR-time* as follows:

$$T^{rel}_{zeroPR} = \frac{T_{zeroPR}}{T_{down}}. \tag{2.8}$$

Ideally, of course, $T^{rel}_{zeroPR} = 1$, i.e., no production takes place exactly during the same time as the downtime. In reality, however, $T^{rel}_{zeroPR} > 1$, because during the transients either buffer b_N may become empty or the machines may not be assigned to process parts from b_N. Therefore, T^{rel}_{zeroPR} quantifies disruptions in the production rate due to transients.

Although the above performance measures do characterize essential features of transients, they do not address, perhaps, the most important one: the variability of $WIP(n)$ and $PR(n)$. To introduce appropriate metrics, we use the notion of *total variation of a function* [25]. For a differentiable function $f(t),\ t \in [a, b]$, the total variation can be calculated as

$$V(f) = \int_a^b |f'(t)|\ dt.$$

For the discrete time functions $WIP(n)$ and $PR(n)$, we re-formulate the above expression as

$$V(WIP) = \sum_{n=n_0+1}^{n_0+T_{down}+T_s} |WIP(n) - WIP(n-1)|\,,\ V(PR) = \sum_{n=n_0+1}^{n_0+T_{down}+T_s} |PR(n) - PR(n-1)|\,, \qquad (2.9)$$

where n_0, as before, is the time slot when the machine(s) went down. We use (2.9) as the measures of *variability* of WIP and PR induced by the downtime.

Investigation of the trajectories of (2.1) and performance measures (2.3)-(2.9) is the topic of this work.

2.2.2 Equations for buffer-based priority dispatch

Equations (2.1) can be further specialized for various dispatch policies. To accomplish this for *buffer-based priority* disciplines, such as FBFS or LBFS, let $\pi(i) \in \{1, 2, \ldots, N\}$ denote the priority of buffer b_i as far as machine allocations are concerned. Clearly, for FBFS, $\pi(1) = 1,\ \pi(2) = 2, \ldots,\ \pi(N) = N$, while for LBFS, $\pi(1) = N,\ \pi(2) = N-1, \ldots,\ \pi(N) = 1$. Let $S_i(n),\ i = 0, 1, \ldots, N$, denote the number of machines allocated at the beginning of slot n to the buffers of priority higher than b_i, i.e., $S_i(n) = \sum_{j:\pi(j)<\pi(i)} v_j(n)$. Then, the machine allocation for buffer b_i can be expressed as

$$v_i(n) = \min\{x_i(n), M'(n) - S_i(n)\},\ i = 1, 2, \ldots, N, \qquad (2.10)$$

where $M'(n) \leqslant M$ is the number of machines that are up at time slot n. Obviously, $v_i(n)$ depends on $x_i(n)$ and, through S_i, on other x_j's with the priorities higher than b_i, e.g.,

$$v_i(n) = v_i(x_1(n), x_2(n), \ldots, x_i(n)),\ i = 1, 2, \ldots, N \text{ for FBFS},$$

$$v_i(n) = v_i(x_i(n), x_{i+1}(n), \ldots, x_N(n)),\ i = 1, 2, \ldots, N \text{ for LBFS}.$$

Then, with a slight abuse of notations, for any buffer-based priority dispatch, equations (2.1) can be re-written as

$$
\begin{aligned}
x_1(n+1) =& x_1(n) + r - v_1(x_1(n), x_2(n), \ldots, x_N(n)),\\
x_i(n+1) =& x_i(n) + v_{i-1}(x_1(n-\tau_{i-1}), x_2(n-\tau_{i-1}), \ldots, x_N(n-\tau_{i-1})) -\\
& v_i(x_1(n), x_2(n), \ldots, x_N(n)),\ i = 2, 3, \ldots, N.
\end{aligned}
\tag{2.11}
$$

Clearly, these delay-difference equations can be represented in the extended form, similar to the difference equations (2.2), i.e.,

$$
\begin{aligned}
z_{01}(n+1) &= r,\\
z_{0j}(n+1) &= z_{0,j-1}(n),\ j = 2, 3, \ldots, \tau_0,\\
x_1(n+1) &= x_1(n) + z_{0,\tau_0}(n) - v_1(x_1(n), x_2(n), \ldots, x_N(n)),\\
z_{i1}(n+1) &= v_i(x_1(n), x_2(n), \ldots, x_N(n)),\ i = 1, 2, \ldots, N-1,\\
z_{ij}(n+1) &= z_{i,j-1}(n),\ i = 1, 2, \ldots, N-1,\ j = 2, 3, \ldots, \tau_i,\\
x_i(n+1) &= x_i(n) + z_{i-1,\tau_{i-1}}(n) - v_i(x_1(n), x_2(n), \ldots, x_N(n)),\ i = 2, 3, \ldots, N,\\
z_{N1}(n+1) &= v_N(x_1(n), x_2(n), \ldots, x_N(n)),\\
z_{Nj}(n+1) &= z_{N,j-1}(n),\ j = 2, 3, \ldots, \tau_N.
\end{aligned}
\tag{2.12}
$$

These equations are the basis for analysis throughout this paper.

2.2.3 Nature of nonlinearities

Obviously, (2.12) is a system of nonlinear equations. What kind of nonlinearities do they involve? To answer this question, consider the simplest case of a system with $M = 4$, $N = 2$, $\tau_1 = 1$, $\tau_0 = \tau_2 = 0$ under, say, FBFS dispatch. Then, equations (2.12) become (see Figure 2.2(a)):

- In Region 1, defined by $x_1 + x_2 < M$,

$$
x_1(n+1) = r,\ x_2(n+1) = x_1(n-1); \tag{2.13}
$$

- In Region 2, defined by $x_1 < M$ and $x_1 + x_2 > M$,

$$x_1(n+1) = r,\ x_2(n+1) = x_2(n) + x_1(n-1) - (M - x_1(n)); \tag{2.14}$$

- In Region 3, defined by $x_1 > M$,

$$x_1(n+1) = x_1(n) + r - M,\ x_2(n+1) = x_2(n) + M. \tag{2.15}$$

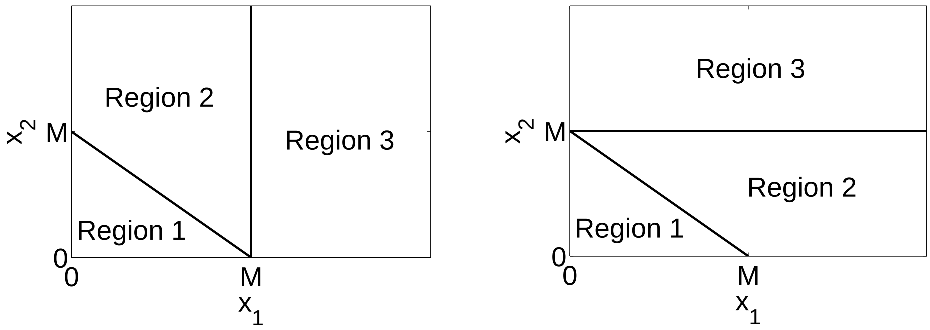

(a) FBFS dispatch (b) LBFS dispatch

Figure 2.2: Linearity regions

Similar equations can be written for LBFS dispatch as well (see Figure 2.2(b), where the corresponding regions are indicated). Also, equations (2.13)-(2.15) can be generalized for arbitrary values of M, N, and τ_i. Although, in general, there are $N+1$ regions of linearity: Region 1 for both FBFS and LBFS is defined by

$$\sum_{i=1}^{N} x_i < M, \tag{2.16}$$

and Region s, $s = 2, 3, \ldots, N+1$, by

$$\sum_{i=1}^{N-s+2} x_i > M,\ \sum_{i=1}^{N-s+1} x_i < M \text{ for FBFS,} \tag{2.17}$$

$$\sum_{i=s-1}^{N} x_i > M,\ \sum_{i=s}^{N} x_i < M \text{ for LBFS.} \tag{2.18}$$

The important regions for our analyses are Regions 1 and 2. They have an important role for the analyses described in Sections 3 and 4.

Since equations (2.13)-(2.15) are linear, we conclude that the nature of nonlinear equations (2.12) is, in fact, piece-wise linear: In each region, the system behaves as a linear one, and the nonlinear behavior arises due to transitions from one region to another. The eigenvalues of the *constituent* linear equations, i.e., equations acting in each linearity region, can be readily calculated (see (A.8), (A.9), and (A.10) in the Appendix). However, as it is well known [26], the eigenvalues of piece-wise linear systems may not characterize the overall system stability. Therefore, the fact that (2.12) is piece-wise linear does not offer an immediate simplification for their global stability and transient analyses.

2.3 Problems considered

The problems addressed in this paper are:

- Determine the equilibria of the re-entrant lines modeled by assumptions (i)-(vii) under the FBFS and LBFS dispatch policies.
- Analyze the stability of these steady states.
- Investigate transients of re-entrant lines in terms of performance measures (2.3)-(2.9).
- Characterize advantages and disadvantages of FBFS and LBFS from these points of view.

Solutions of these problems are described in Sections 3-8 below.

3 Steady States

3.1 Approach

Consider the system described by equations (2.12) and denote its steady state by

$$\boldsymbol{X}_{ss} := [(\boldsymbol{x}^{ss})^T, (\boldsymbol{z}_{\boldsymbol{0}}^{ss})^T, (\boldsymbol{z}_{\boldsymbol{1}}^{ss})^T, \dots, (\boldsymbol{z}_N^{ss})^T]^T, \tag{3.1}$$

where

$$\boldsymbol{x}^{ss} = [x_1^{ss}, x_2^{ss}, \dots, x_N^{ss}]^T,\ \boldsymbol{z}_{\boldsymbol{i}}^{ss} = [z_{i1}^{ss}, z_{i2}^{ss}, \dots, z_{i,\tau_i}^{ss}]^T,\ i = 0, 1, \dots, N. \tag{3.2}$$

In this section, we first provide a necessary condition for a re-entrant line under any dispatch policy to have an equilibrium point. Then, we formulate conditions for uniqueness and for multiplicity of equilibria under FBFS and LBFS dispatch. Finally, we comment on the regions, where these equilibria are located.

3.2 A necessary condition for existence of equilibria

Theorem 3.1 *Under any dispatch policy, the re-entrant line defined by assumptions (i)-(vii) has an equilibrium only if*

$$r \leqslant \frac{M}{N}. \tag{3.3}$$

In the proof of this theorem, it is shown (see (A.4) in the Appendix) that, if a steady state exists, the z-part of (3.1), i.e., $\boldsymbol{z}_i^{ss} = [z_{i1}^{ss}, z_{i2}^{ss}, \dots, z_{i,\tau_i}^{ss}]^T$, is given by

$$\boldsymbol{z}_i^{ss} = [z_{i1}^{ss} = r, z_{i2}^{ss} = r, \dots, z_{i,\tau_i}^{ss} = r]^T, \ i = 0, 1, \dots, N. \tag{3.4}$$

Because of that, we address below only the x-part of (3.1), i.e., $\boldsymbol{x}^{ss} = [x_1^{ss}, x_2^{ss}, \dots, x_N^{ss}]^T$.

3.3 Necessary and sufficient conditions for uniqueness and for multiplicity of steady states

Theorem 3.2 *The re-entrant line defined by assumptions (i)-(vii) has:*

(a) a unique equilibrium

$$\boldsymbol{x}^{ss} = [x_1^{ss} = r, x_2^{ss} = r, \dots, x_N^{ss} = r]^T \tag{3.5}$$

for either FBFS or LBFS dispatch if and only if

$$r < \frac{M}{N}; \tag{3.6}$$

(b) multiple (countable) equilibria

$$\boldsymbol{x}^{ss} = [x_1^{ss} = r, x_2^{ss} = r, \dots, x_{N-1}^{ss} = r, x_N^{ss} = q]^T, \ q \geqslant r \text{ for FBFS}, \tag{3.7}$$

$$\boldsymbol{x}^{ss} = [x_1^{ss} = q, x_2^{ss} = r, \ldots, x_{N-1}^{ss} = r, x_N^{ss} = r]^T,\ q \geqslant r \textit{ for LBFS} \tag{3.8}$$

if and only if

$$r = \frac{M}{N}. \tag{3.9}$$

Note that under condition (3.6), the unique equilibrium (3.5) satisfies the inequality

$$\sum_{i=1}^{N} x_i^{ss} = Nr < M, \tag{3.10}$$

which implies that it is located in the interior of Region 1 (see (2.16) and Figure 2.2) under both FBFS and LBFS disciplines. On the other hand, under condition (3.9), the multiple equilibria (3.7) and (3.8) satisfy

$$\sum_{i=1}^{N} x_i^{ss} = (N-1)r + q \geqslant M,\ \sum_{i=1}^{N-1} x_i^{ss} = (N-1)r < M \text{ for FBFS}, \tag{3.11}$$

$$\sum_{i=1}^{N} x_i^{ss} = (N-1)r + q \geqslant M,\ \sum_{i=2}^{N} x_i^{ss} = (N-1)r < M \text{ for LBFS}, \tag{3.12}$$

implying that these equilibria are in the closed Region 2 (see (2.17), (2.18), and Figure 2.2). Thus, there are no equilibria outside of Regions 1 and 2 for either FBFS or LBFS.

4 Stability

4.1 Approach

The stability property addresses the issue of system returning to a steady state from initial conditions away from the equilibria. Thus, one must specify which steady state is addressed and then investigate its stability. As it is shown above, the re-entrant line under consideration has either unique steady state (3.5) or multiple equilibria (3.7), (3.8). As far as multiple equilibria (3.7), (3.8) are concerned, the situation is quite simple:

Theorem 4.1 *Equilibria (3.7) and (3.8) are not attractive in the sense that the trajectories do not return to these equilibria under any initial deviation.*

The analysis of stability properties of equilibrium (3.5) is more involved. Therefore, first, we show that it is finite-time stable, i.e., reaches the equilibrium from initial conditions close enough to the steady state within a finite time interval. Then, we address the issue of global convergence to (3.5) from any non-negative initial condition. It turns out that it is globally attractive for FBFS, while for LBFS, it is not. However, we establish a numerical fact, which indicates that if the delays in all re-entrant paths are identical, equilibrium (3.5) is globally attractive under LBFS as well.

4.2 Stability properties of the unique steady state

Theorem 4.2 *Steady state (3.5) of the re-entrant line defined by assumptions (i)-(vii) is (locally) finite-time stable for both FBFS and LBFS dispatch policies.*

Theorem 4.3 *For FBFS dispatch, steady state (3.5) of the re-entrant line defined by assumptions (i)-(vii) is globally attractive.*

An illustration of Theorem 4.3 is given in Figures 4.1-4.3 for the system with

$$M = 5,\ N = 4,\ \tau_0 = \tau_4 = 0,\ \tau_1 = 7,\ \tau_2 = 18,\ \tau_3 = 34,\ r = 1 \tag{4.1}$$

and three sets of initial conditions:

$$\begin{gathered} x_i(0) = 2,\ i = 1,2,3,4;\ z_{i1}(0) = 0,\ i = 1,2,3; \\ z_{ij}(0) = 1,\ i = 1,2,3,\ j = 2,3,\dots,\tau_i; \end{gathered} \tag{4.2}$$

$$\begin{gathered} x_i(0) = 5,\ i = 1,2,3,4;\ z_{ij}(0) = 0,\ i = 1,2,3,\ j = 1,2,3,4; \\ z_{ij}(0) = 1,\ i = 1,2,3,\ j = 5,6,\dots,\tau_i; \end{gathered} \tag{4.3}$$

$$\begin{gathered} x_i(0) = 6,\ i = 1,2,3,4;\ z_{ij}(0) = 0,\ i = 1,2,3,\ j = 1,2,\dots,5; \\ z_{ij}(0) = 1,\ i = 1,2,3,\ j = 6,7,\dots,\tau_i. \end{gathered} \tag{4.4}$$

Note that system (4.1) has the unique steady state at

$$\boldsymbol{X}_{ss} = [1,1,\dots,1]^T. \tag{4.5}$$

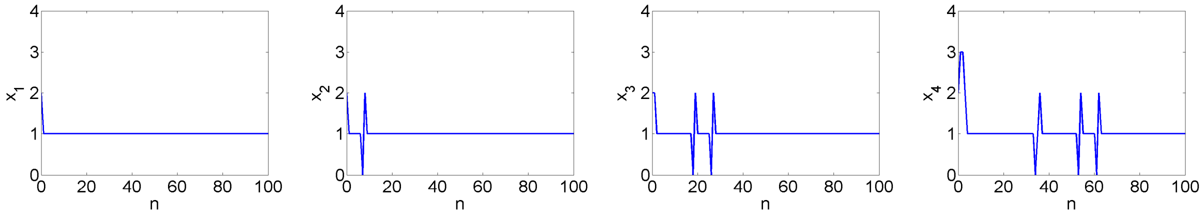

(a) For initial conditions (4.2)

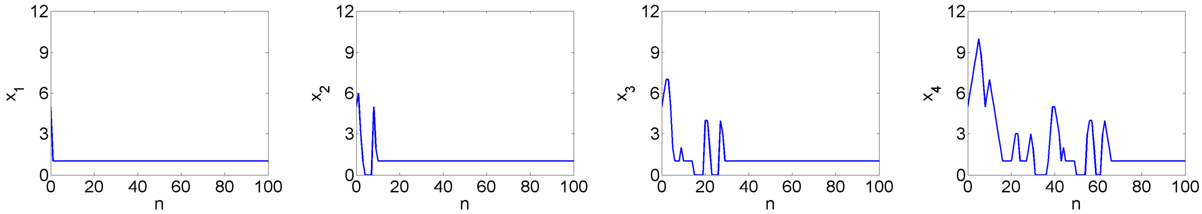

(b) For initial conditions (4.3)

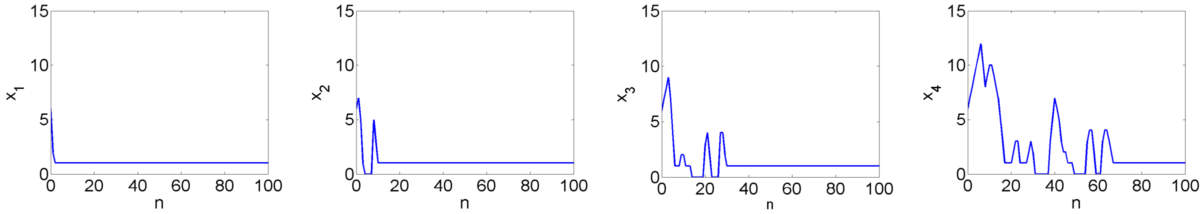

(c) For initial conditions (4.4)

Figure 4.1: State trajectories of system (4.1) under FBFS

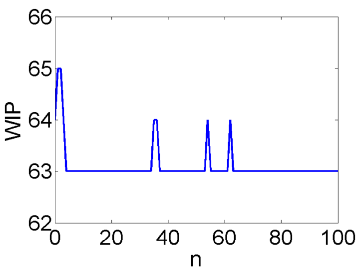

(a) For initial condition (4.2)

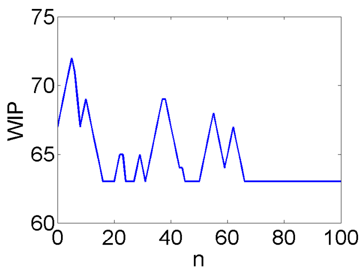

(b) For initial condition (4.3)

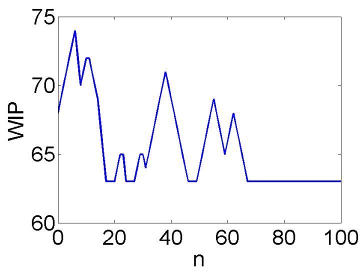

(c) For initial condition (4.4)

Figure 4.2: *WIP* trajectories of system (4.1) under FBFS

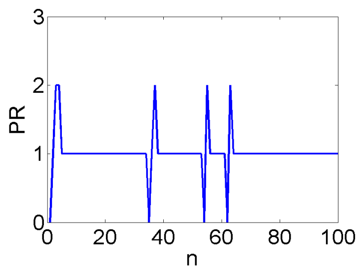

(a) For initial condition (4.2)

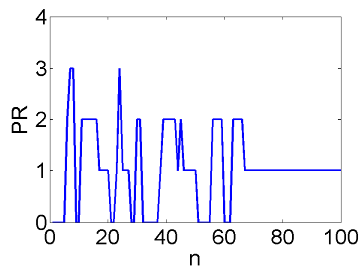

(b) For initial condition (4.3)

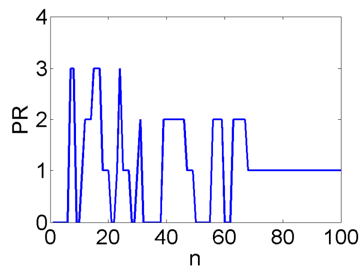

(c) For initial condition (4.4)

Figure 4.3: *PR* trajectories of system (4.1) under FBFS

Numerical Fact 4.1 *For LBFS dispatch, steady state (3.5) of the re-entrant line defined by assumptions (i)-(vii) is not globally attractive.*

Justification: To justify this fact, consider the re-entrant line (4.1) and initial conditions (4.2)-(4.4). Solving the corresponding difference equations (2.12), we observe the following three patterns of behavior:

(a) When the initial condition is close enough to equilibrium (4.5), (i.e., initial condition (4.2)), the system converges to the steady state. This, of course, is predicted by Theorem 4.2 and is illustrated in Figures 4.4(a), 4.5(a), and 4.6(a).

(b) When the initial condition is further away from equilibrium (4.5), (i.e., (4.3)), the system converges to a periodic regime. This is illustrated in Figures 4.4(b), 4.5(b), and 4.6(b).

(c) When the initial condition is still further away from the equilibrium (i.e., (4.4)), the system converges to an oscillatory but aperiodic regime. This is illustrated in Figures 4.4(c), 4.5(c), and 4.6(c). Although this regime can be analyzed in details using the theory of chaotic systems [27], we defer this analysis to future work and refer to this behavior as *chaotic*.

Thus, in general, LBFS does not ensure global convergence. However, if the delays in all re-entrant paths are the same, i.e., $\tau_i = \tau$, $i = 1, 2, \ldots, N-1$, the situation is different. To simplify the investigation of this case, we need the following auxiliary statement:

Lemma 4.1 *Assume that equilibrium (3.5) of a re-entrant line defined by assumptions (i)-(vii) with $\tau_0 = \tau_N = 0$ is globally attractive. Then, it remains globally attractive for any $\tau_0 > 0$ and $\tau_N > 0$.*

Based on this lemma, we study below systems with $\tau_0 = \tau_N = 0$. Specifically, we consider 315 re-entrant lines with LBFS dispatch, $\tau_i = \tau$, $i = 1, 2, \ldots, N-1$, and the parameters selected as all possible combinations of the following sets:

$$N \in \{2, 3, 4, 5, 10, 15, 20\},\ \tau \in \{2, 5, 7, 18, 34\},\ r \in \{1, 2, 3\},\ E \in \{1, 2, 3\}, \tag{4.6}$$

where $E = M - Nr$ is the *extra capacity* of the bottleneck workcenter. For each of the systems, thus constructed, we considered 1000 initial conditions with x_i, $i = 1, 2, \ldots, N$, and z_{ij}, $i = 1, 2, \ldots, N-1$, $j = 1, 2, \ldots, \tau_i$, selected randomly, equiprobably, and independently from the set $\{0, 1, \ldots, 20\}$. Solving the resulting $315,000$ systems of equations (2.12), we obtained:

Numerical Fact 4.2 *For all* 315 *systems analyzed, the trajectories reached steady state (3.5) within a finite time for every initial condition selected.*

To illustrate this fact, equations (2.12) of the system

$$M = 5,\ N = 4,\ \tau_0 = \tau_4 = 0,\ \tau_i = 18,\ i = 1, 2, 3,\ r = 1 \tag{4.7}$$

and initial conditions (4.2)-(4.4) under LBFS are solved, and the state trajectories, *WIP* trajectories, and *PR* trajectories are shown in Figures 4.7-4.9.

Based on Numerical Fact 4.2, we hypothesize that (3.5) is finite-time globally attractive for LBFS dispatch if $\tau_i = \tau$, $i = 1, 2, \ldots, N-1$.

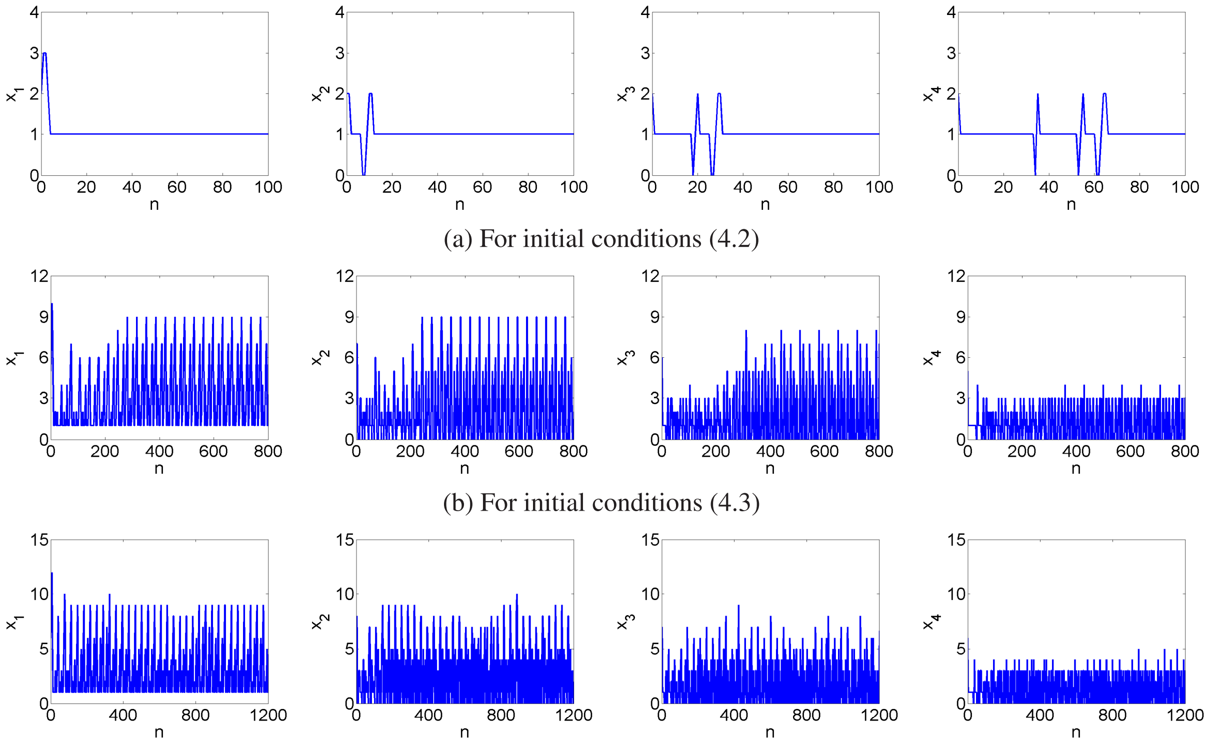

(a) For initial conditions (4.2)

(b) For initial conditions (4.3)

(c) For initial conditions (4.4)

Figure 4.4: State trajectories of system (4.1) under LBFS

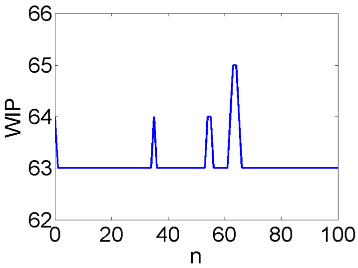

(a) For initial condition (4.2)

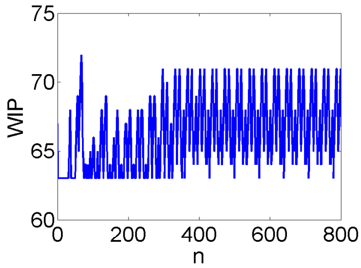

(b) For initial condition (4.3)

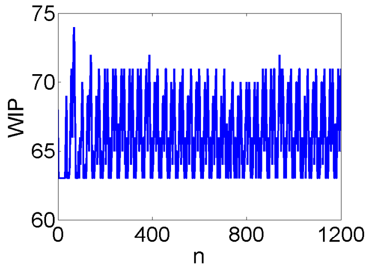

(c) For initial condition (4.4)

Figure 4.5: *WIP* trajectories of system (4.1) under LBFS

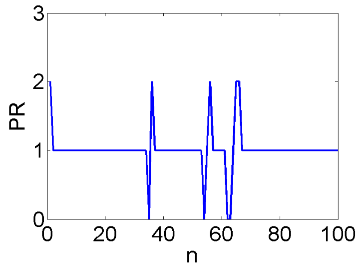

(a) For initial condition (4.2)

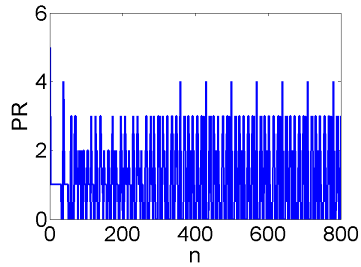

(b) For initial condition (4.3)

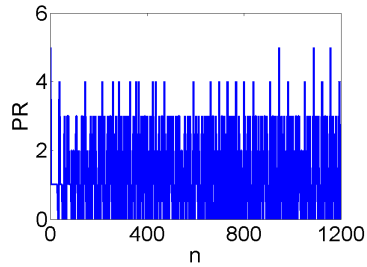

(c) For initial condition (4.4)

Figure 4.6: *PR* trajectories of system (4.1) under LBFS

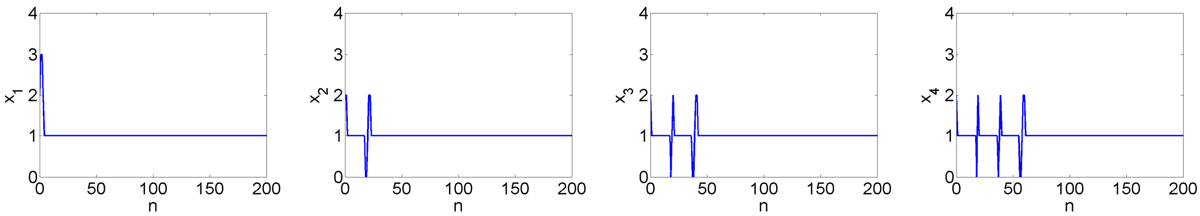

(a) For initial conditions (4.2)

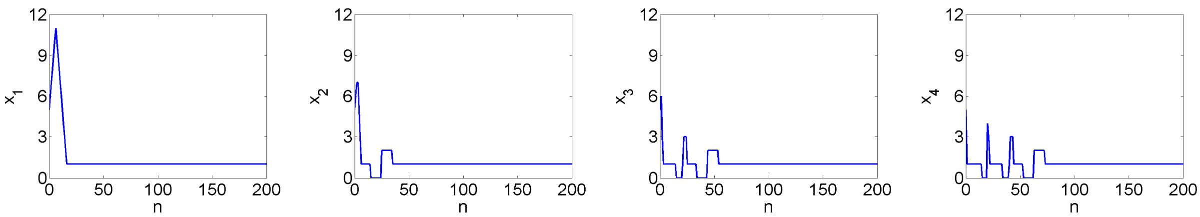

(b) For initial conditions (4.3)

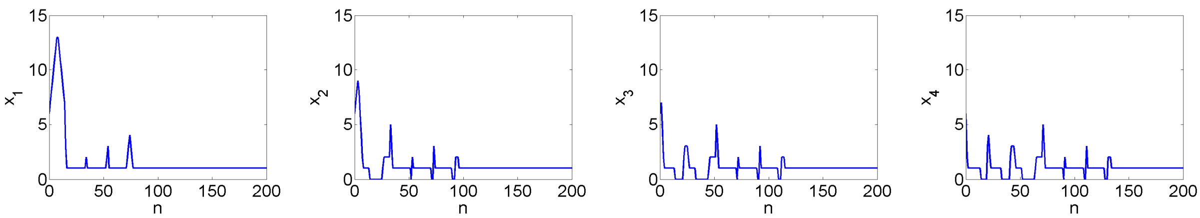

(c) For initial conditions (4.4)

Figure 4.7: State trajectories of system (4.7) under LBFS

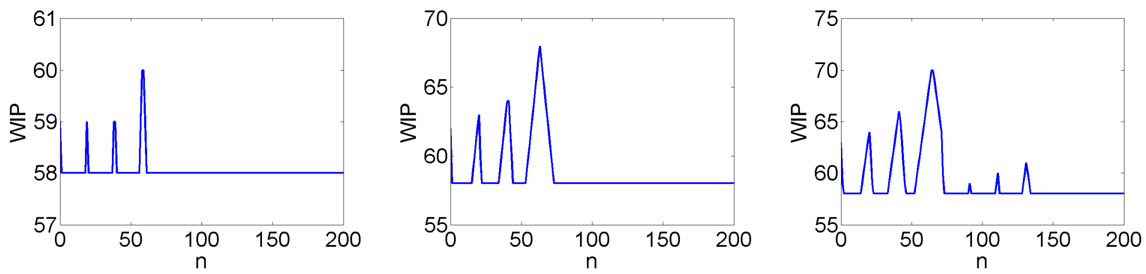

(a) For initial condition (4.2) (b) For initial condition (4.3) (c) For initial condition (4.4)

Figure 4.8: *WIP* trajectories of system (4.7) under LBFS

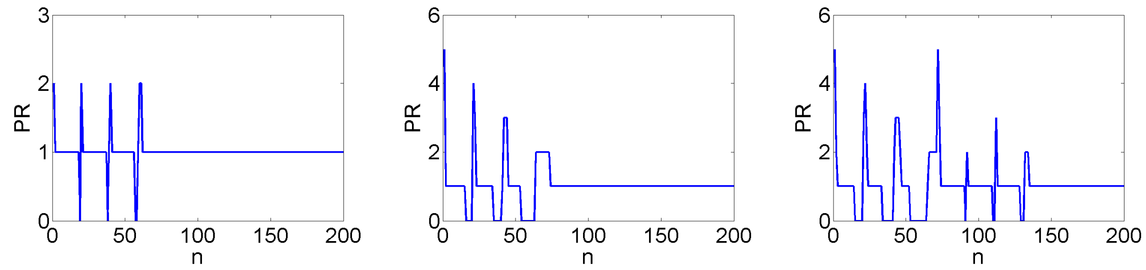

(a) For initial condition (4.2) (b) For initial condition (4.3) (c) For initial condition (4.4)

Figure 4.9: *PR* trajectories of system (4.7) under LBFS

5 Transients under FBFS Dispatch

5.1 Approach

Transients are the processes of reaching steady states of dynamical systems. Obviously, the transients exist only when the system has stable equilibria. Hence, we address here transients of re-entrant lines, which possess a unique globally attractive equilibrium under both FBFS and LBFS, i.e., when

$$r < \frac{M}{N}, \ \tau_i = \tau, \ i = 1, 2, \ldots, N-1$$

and assume, for simplicity, that $\tau_0 = \tau_N = 0$. Generalizations to transients in the case of $\tau_i \neq \tau_j$, $i \neq j$ and $\tau_0 > 0$, $\tau_N > 0$ are provided in Section 8.

Typically, transients in a dynamical system are of infinite duration, i.e., the system reaches its steady state asymptotically, as time tends to infinity. This is due to the fact that, generically, linearizations around equilibria have bounded eigenvalues (in the continuous time case) or eigenvalues away from the origin (in the discrete time case). In the systems under consideration, however, all eigenvalues of the constituent linear system in Region 1 are at the origin for both FBFS and LBFS (see the proof of Theorem 4.2). This implies that the transients are of finite duration. Based on this, we introduce formally the notion of settling time alluded to in Section 2:

Definition 5.1 *The settling time, T_s, of the re-entrant line defined by assumptions (i)-(vii) is the time necessary to reach the globally attractive steady state, starting from the initial condition*

$$\boldsymbol{X}(0) := [x_1(0), \ldots, x_N(0), z_{01}(0), \ldots, z_{0,\tau_0}(0), \ldots, z_{N1}(0), \ldots, z_{N,\tau_N}(0)]^T. \tag{5.1}$$

Clearly, when the state, $\boldsymbol{X}(n)$, reaches its steady state, $\boldsymbol{X}_{ss} = \boldsymbol{X}(T_s)$, the outputs $PR(n)$ and $WIP(n)$ also reach their steady state values PR_{ss} and WIP_{ss}. Thus, the duration and other properties of transients can be studied using either the state $\boldsymbol{X}(n)$ or the outputs $PR(n)$ and $WIP(n)$. Since our goal is the analysis of performance measures (2.3)-(2.9), in this and the subsequent sections, we concentrate on the latter.

According to Definition 5.1, the settling time depends on the initial condition $\boldsymbol{X}(0)$. From this point of view, the following two situations are of importance:

(a) Initially, the system is empty, i.e., all states are at zero: $\boldsymbol{X}(0) = \mathbf{0}$.

(b) Initial states are defined by the machine downtime. In this case, we assume that the system has been operating in steady state (3.5) when one or more machines of the BNWC either experienced a breakdown or stopped for preventive maintenance and remained down for a period of time denoted as T_{down} (in units of the machine cycle time). If during this downtime, condition (3.3) is violated, the system leaves steady state (3.5). At the end of this period, when all machines are operational, the system reaches the state

$$[x_1(T_{down}), \ldots, x_N(T_{down}), z_{01}(T_{down}), \ldots, z_{0,\tau_0}(T_{down}), \ldots, z_{N1}(T_{down}), \ldots, z_{N,\tau_N}(T_{down})]^T, \tag{5.2}$$

and this state is viewed as the initial condition. All initial conditions generated in such a manner are referred to as *downtime-based*.

In this and subsequent sections, we concentrate on the transients from the downtime-based, rather than zero, initial conditions, since the former are more important in practice. Nevertheless, for the sake of completeness, we provide below a simple result on the duration of transients from zero initial conditions:

Theorem 5.1 *Consider the system defined by assumptions (i)-(vii) with either FBFS or LBFS dispatch. Assume that condition (3.3) is satisfied. Then, the settling time, T_s, from zero initial conditions, is given by*

$$T_s = N + \sum_{i=0}^{N} \tau_N. \tag{5.3}$$

Thus, for zero initial conditions, the duration of transients is linearly dependent on the number of re-entrant paths and the delays in each of them. In other words, in systems with many re-entrant paths and long time delays, the settling time can be quite long. An illustration is given in Figure 5.1 where *WIP*(n) and *PR*(n) are plotted for the system defined by

$$M = 16,\ N = 15,\ \tau_i = 29,\ i = 1, 2, \ldots, 14,\ \tau_0 = \tau_{15} = 0,\ r = 1. \tag{5.4}$$

As one can see the behavior is aperiodic and remains the same for practically all systems analyzed.

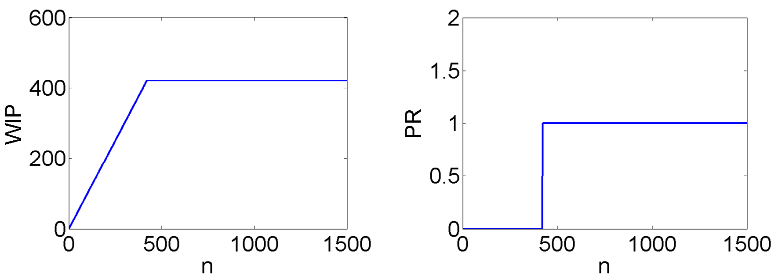

(a) *WIP*(n) (b) *PR*(n)

Figure 5.1: Transients for zero initial condition

Unfortunately, for downtime-based initial conditions, closed formulas for the performance measures introduced in Subsection 2.2 (with the exception T_s) are all but impossible to derive analytically. Therefore, we proceed as follows: First, using extensive numerical studies (by solving equations (2.12)), we investigate qualitative features of the transients of *WIP* and *PR*. Then, we provide empirical quantification of these transients. Finally, we derive analytical results, i.e., closed-form expressions, characterizing the settling time. The current section presents this material for FBFS dispatch; Section 6 is devoted to LBFS; comparisons of the two are provided in Section 7; and several extensions are in Section 8.

5.2 Qualitative characterization

To investigate qualitative properties of transients under FBFS dispatch and downtime-based initial conditions, equations (2.12) have been solved numerically for various values of the model (i)-(vii) parameters, and the results have been represented as trajectories of $WIP(n)$ and $PR(n)$. Typical trajectories are shown in Tables 5.1-5.3 as functions of T_{down} and N for the system with

$$M = Nr + 1, \ \tau = 29 \tag{5.5}$$

and $M' = 0$, i.e., for catastrophic failure of BNWC, which occurs at $n = 101$. From Tables 5.1-5.3, we observe the following:

- Transients of WIP: For $T_{down} \ll \tau$, the transient response of WIP consists of series of spikes, the number of which equals to N; the spikes in each series are of decreasing amplitudes. As T_{down} increases but still remains smaller than τ and r increases, the spikes join together to form a "rippled" bubble. When $T_{down} \geqslant \tau$, the transient response tends to be a triangular waveform.

- Transients of PR: For $T_{down} \ll \tau$, the transient response of PR consists of series of pulses, with positive and negative amplitudes, centered around PR_{ss}. As T_{down} and N increase, the pulses tend to form a triangular sequence. When $T_{down} \geqslant \tau$, the pulses disappear and the transient response is a rectangular waveform. The amplitudes of the pulses range from $-r$ (implying that no production takes place) to a positive number close to $M - r$. For the rectangular waveform, the amplitudes are $-r$ and 1.

Typical transient patterns of $WIP(n)$ and $PR(n)$ are shown in Figures 5.2 and 5.3, respectively. Transients of buffer occupancies for re-entrant line with $N = 2$ are presented in Table 5.4.

Table 5.1: Transients under FBFS ($r = 1$)

(a) Transients of $WIP(n)$

N	T_{down}			
	5	15	30	60
2	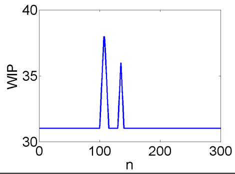	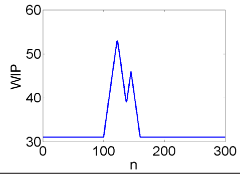	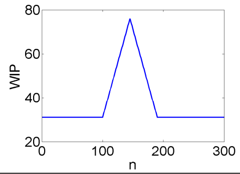	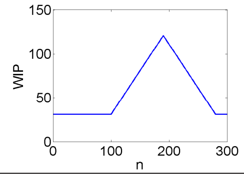
3	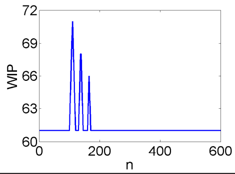	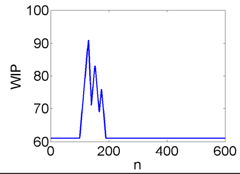	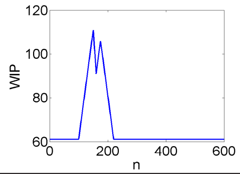	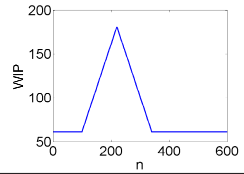
10	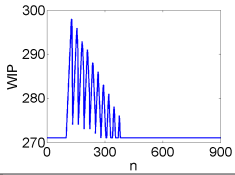	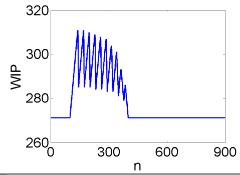	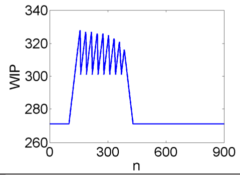	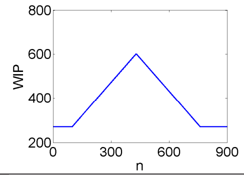
15	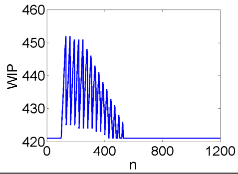	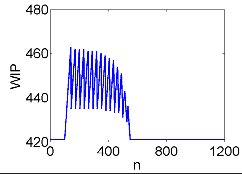	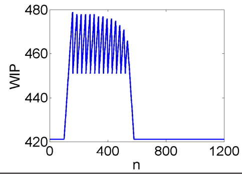	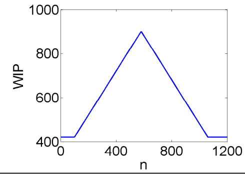

(b) Transients of $PR(n)$

N	T_{down}			
	5	15	30	60
2	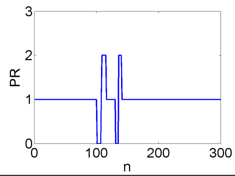	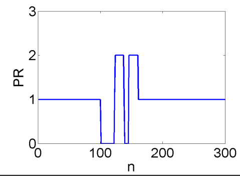	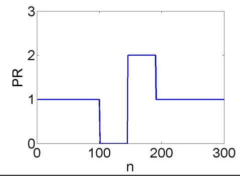	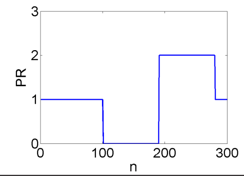
3	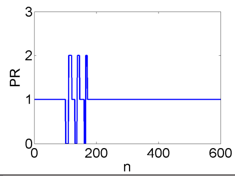	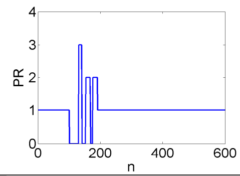	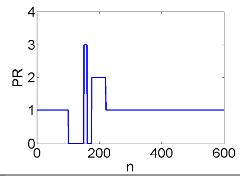	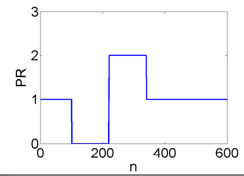
10	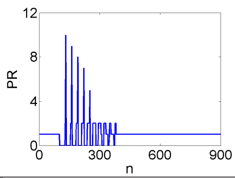	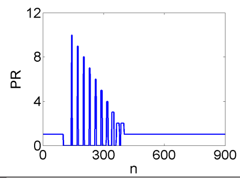	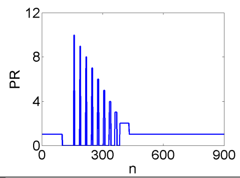	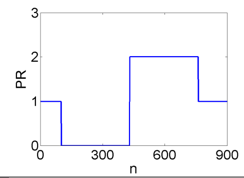
15	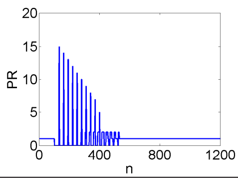	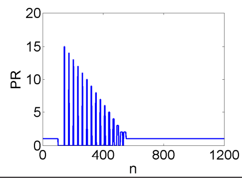	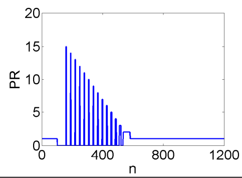	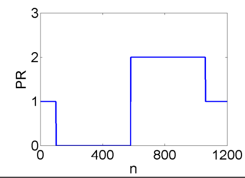

Table 5.2: Transients under FBFS ($r = 2$)

(a) Transients of $WIP(n)$

N	T_{down}			
	5	15	30	60
2	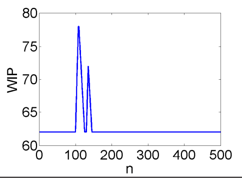	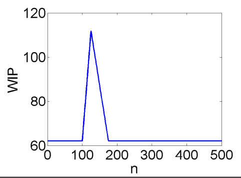	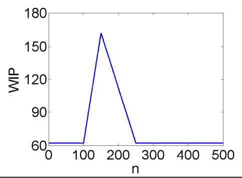	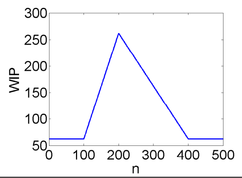
3	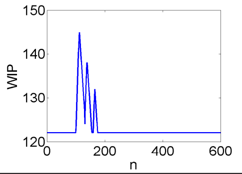	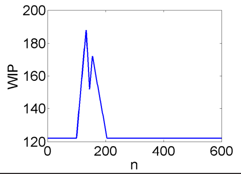	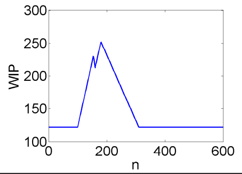	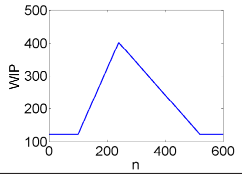
10	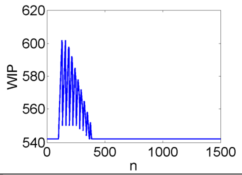	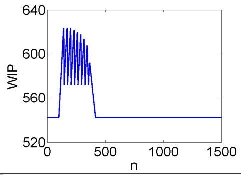	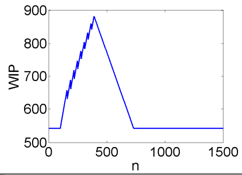	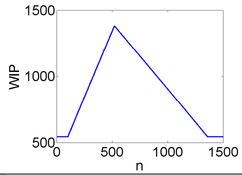
15	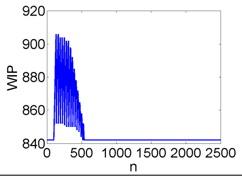	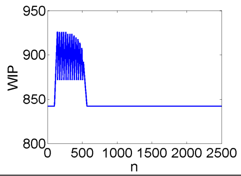	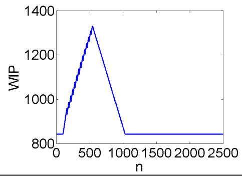	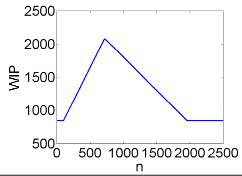

(b) Transients of $PR(n)$

N	T_{down}			
	5	15	30	60
2	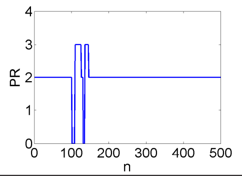	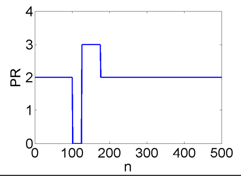	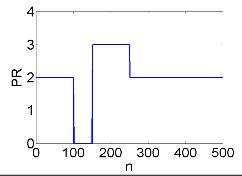	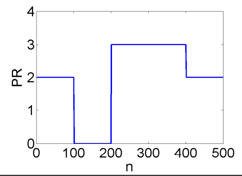
3	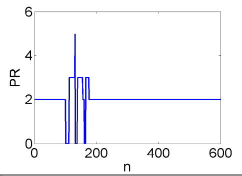	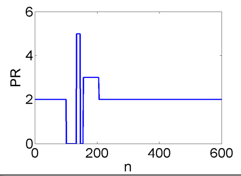	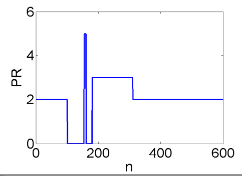	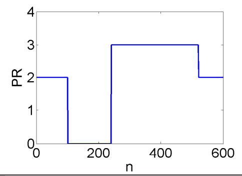
10	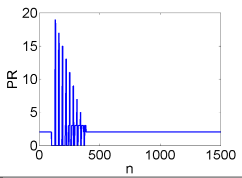	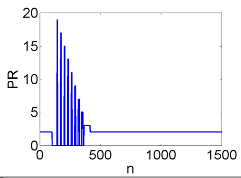	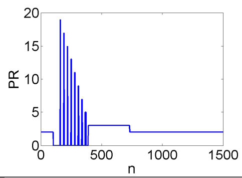	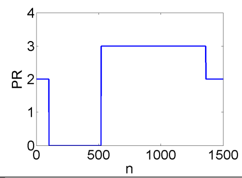
15	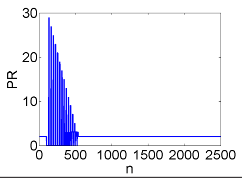	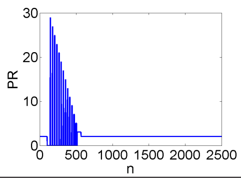	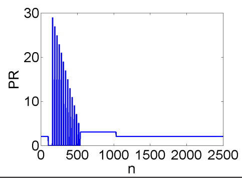	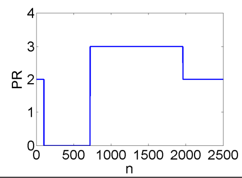

Table 5.3: Transients under FBFS (r = 3)

(a) Transients of $WIP(n)$

N	T_{down} = 5	T_{down} = 15	T_{down} = 30	T_{down} = 60
2	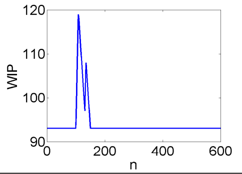	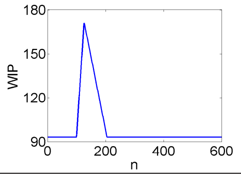	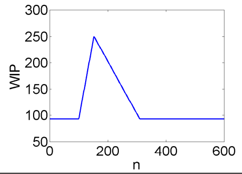	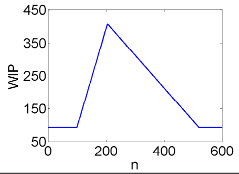
3	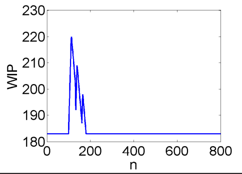	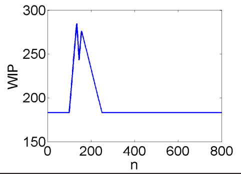	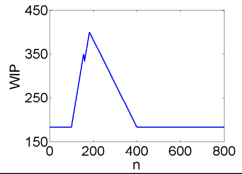	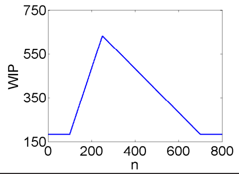
10	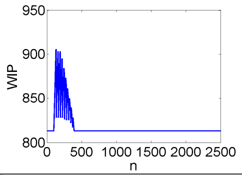	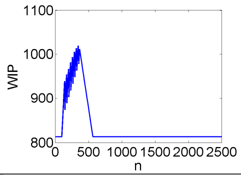	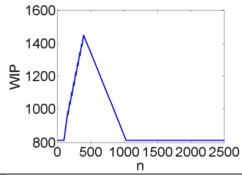	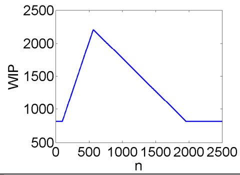
15	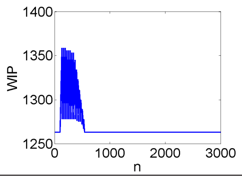	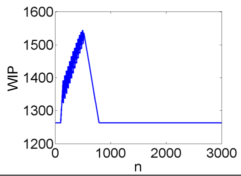	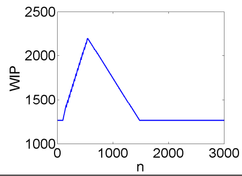	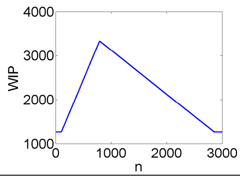

(b) Transients of $PR(n)$

N	T_{down} = 5	T_{down} = 15	T_{down} = 30	T_{down} = 60
2	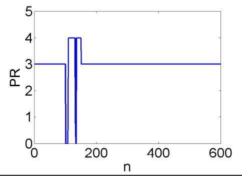	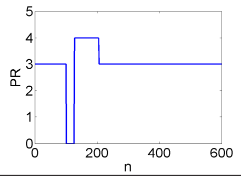	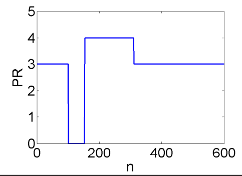	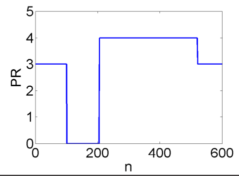
3	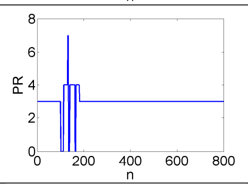	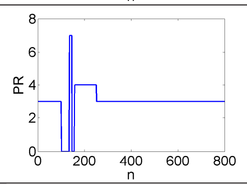	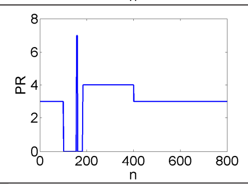	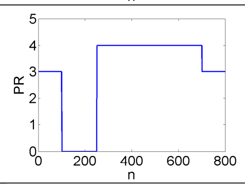
10	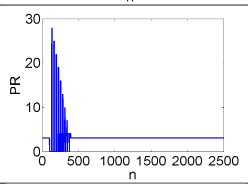	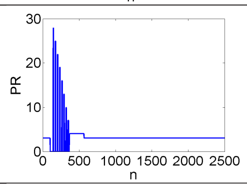	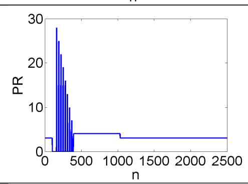	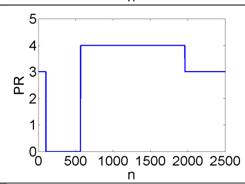
15	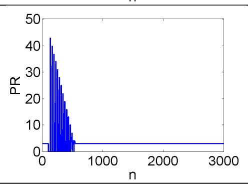	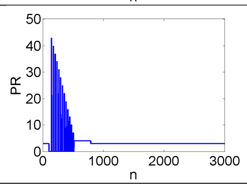	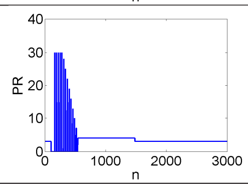	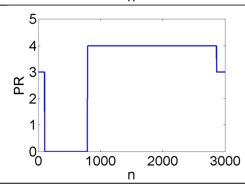

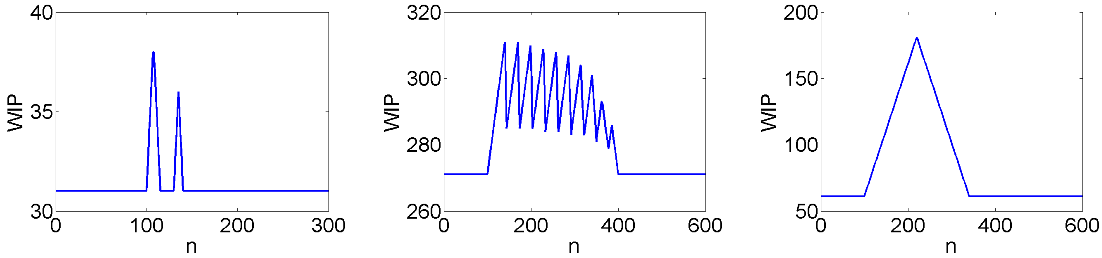

(a) Spikes (b) Rippled bubble (c) Triangular waveform

Figure 5.2: Typical transient patterns for *WIP*(n) under FBFS

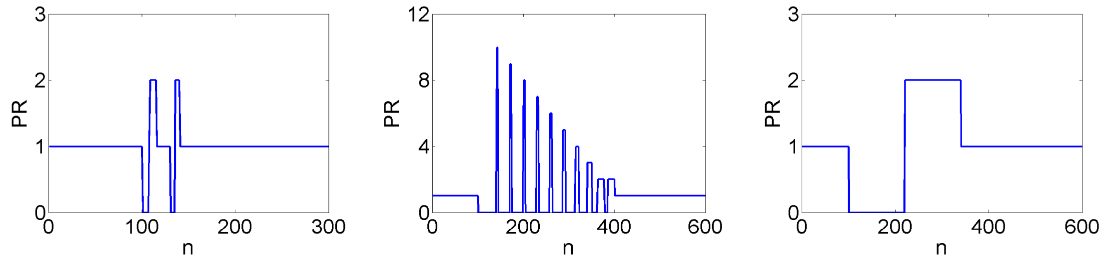

(a) Pulses (b) Triangular series of pulses (c) Rectangular waveform

Figure 5.3: Typical transient patterns for *PR*(n) under FBFS

Table 5.4: Transients under FBFS ($N = 2$)

(a) Transients of $x_1(n)$ and $x_2(n)$ ($r = 1$)

x	T_{down} 5	15	30	60
x_1	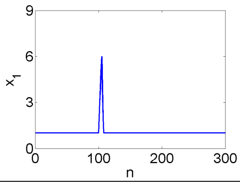	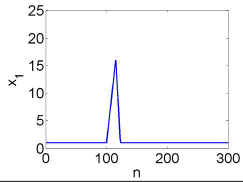	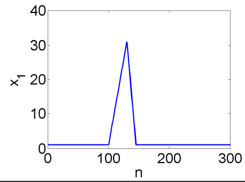	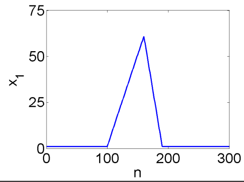
x_2	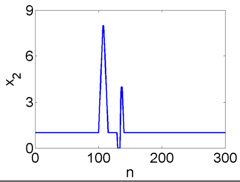	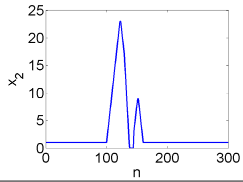	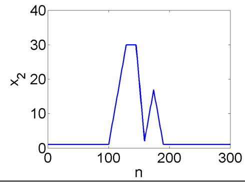	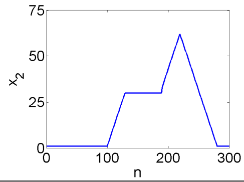

(b) Transients of $x_1(n)$ and $x_2(n)$ ($r = 2$)

x	T_{down} 5	15	30	60
x_1	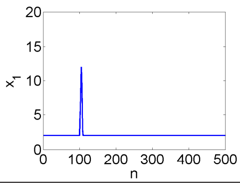	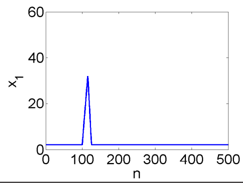	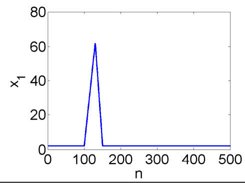	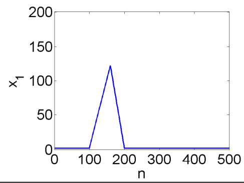
x_2	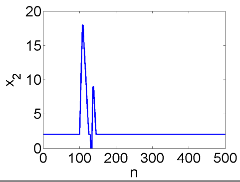	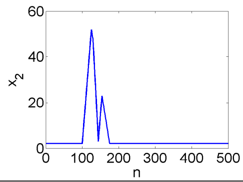	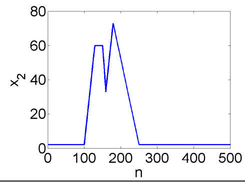	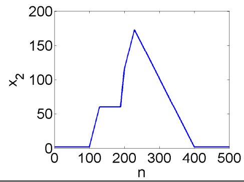

(c) Transients of $x_1(n)$ and $x_2(n)$ ($r = 3$)

x	T_{down} 5	15	30	60
x_1	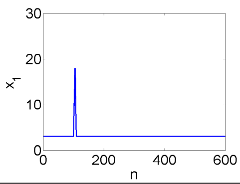	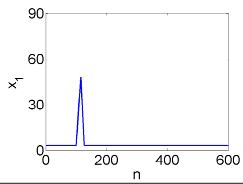	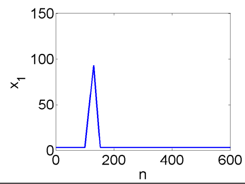	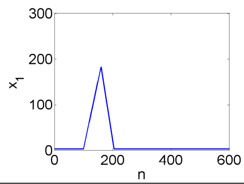
x_2	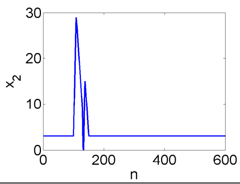	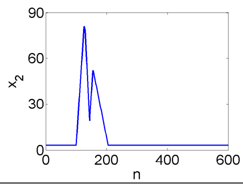	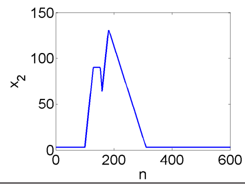	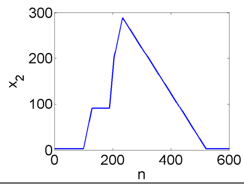

5.3 Empirical quantitative characterization

Based on the data of Tables 5.1-5.3, the transient characteristics (2.3)-(2.9) are quantified in Tables 5.5-5.7. From these tables we conclude:

- Relative settling time, T_s^{rel}: Can be as small as 2 and as large as 87; monotonically increasing in N and r and monotonically decreasing (non-strictly) in T_{down}.
- Excess of *WIP*, EX_{WIP}: Can be as small as 3% and as large as 170%; monotonically decreasing in N and monotonically increasing in r and T_{down}.
- Overshoot of *RT*, OS_{RT}: Can be as small as 7% and as large as 340%; monotonically decreasing in N, monotonically increasing (non-strictly) in r, and monotonically increasing in T_{down}.
- Relative zero-*PR*-time, T_{zeroPR}^{rel}: Can be as small as 1.5 and as large as 59; monotonically increasing in N and in general, monotonically decreasing (non-strictly) in T_{down}.
- Variability of *WIP*, $V(WIP)$: Can be as small as 24 and as large as 4140; monotonically increasing in N, r, and T_{down}.
- Variability of *PR*, $V(PR)$: Can be as small as 4 and as large as 666; monotonically increasing (non-strictly) in N, monotonically increasing (non-strictly, sometimes non-monotonic convex) in r, and monotonically decreasing (non-strictly, sometimes non-monotonic concave) in T_{down}. Note that $V(PR) \ll V(WIP)$.

It is important to note that since *WIP* returns to its steady state after T_s, the average value of $PR(n)$ over the period $T_{down} + T_s$ equals to PR_{ss}, i.e., on average, *there are no production losses due to transients*. Thus, under condition (3.6), i.e., for an under-loaded system, the *detriments of the transients are in creating pulsating throughput, leading to excessive WIP and long RT*.

Table 5.5: Quantification of transients under FBFS ($r = 1$)

(a) T_s^{rel}

N	T_{down} 5	15	30	60
2	7.0	3.0	2.0	2.0
3	13.0	5.0	3.0	3.0
10	55.0	19.0	10.0	10.0
15	85.0	29.0	15.0	15.0

(b) EX_{WIP}

N	T_{down} 5	15	30	60
2	6.5	36.3	72.6	145.2
3	4.2	23.2	44.1	98.4
10	3.4	8.1	13.6	60.9
15	2.8	5.7	9.3	57.0

(c) OS_{RT}

N	T_{down} 5	15	30	60
2	22.6	71.0	145.2	290.3
3	16.4	49.2	82.0	196.7
10	10.0	14.8	21.0	121.8
15	7.4	10.0	13.8	114.0

(d) T_{zeroPR}^{rel}

N	T_{down} 5	15	30	60
2	2.4	1.9	1.5	1.5
3	4.4	3.3	2.2	2.0
10	29.8	14.7	8.0	5.5
15	56.6	23.7	12.5	8.0

(e) $V(WIP)$

N	T_{down} 5	15	30	60
2	24	58	90	180
3	44	98	130	240
10	298	440	480	660
15	566	710	752	960

(f) $V(PR)$

N	T_{down} 5	15	30	60
2	8	8	4	4
3	12	14	10	4
10	98	112	108	4
15	228	242	238	4

Table 5.6: Quantification of transients under FBFS ($r = 2$)

(a) T_s^{rel}

N	T_{down} 5	15	30	60
2	8.0	4.0	4.0	4.0
3	14.0	6.0	6.0	6.0
10	56.0	20.0	20.0	20.0
15	86.0	30.0	30.0	30.0

(b) EX_{WIP}

N	T_{down} 5	15	30	60
2	10.1	40.3	80.6	161.3
3	7.4	25.9	55.3	114.8
10	4.4	8.7	32.7	77.5
15	3.3	6.0	30.0	73.6

(c) OS_{RT}

N	T_{down} 5	15	30	60
2	25.8	80.6	161.3	322.6
3	19.7	54.1	106.6	229.5
10	11.1	15.1	62.7	155.0
15	7.6	10.0	58.2	147.3

(d) T_{zeroPR}^{rel}

N	T_{down} 5	15	30	60
2	2.6	1.7	1.7	1.7
3	4.6	2.9	2.5	2.3
10	32.8	14.3	8.8	7.0
15	59.2	23.3	13.4	10.3

(e) $V(WIP)$

N	T_{down} 5	15	30	60
2	52	100	200	400
3	94	172	296	560
10	662	856	1052	1680
15	1192	1396	1614	2480

(f) $V(PR)$

N	T_{down} 5	15	30	60
2	12	6	6	6
3	22	16	16	6
10	204	198	198	6
15	454	448	448	6

Table 5.7: Quantification of transients under FBFS ($r = 3$)

(a) T_s^{rel}

N	T_{down} 5	15	30	60
2	9.0	6.0	6.0	6.0
3	15.0	9.0	9.0	9.0
10	57.0	30.0	30.0	30.0
15	87.0	45.0	45.0	45.0

(b) EX_{WIP}

N	T_{down} 5	15	30	60
2	12.9	42.3	84.7	169.4
3	9.3	28.8	60.3	123.0
10	4.8	14.5	39.8	85.8
15	3.5	12.5	37.5	81.9

(c) OS_{RT}

N	T_{down} 5	15	30	60
2	29.0	83.9	171.0	338.7
3	21.3	55.7	119.7	245.9
10	11.4	25.5	78.6	171.6
15	7.6	22.3	62.9	163.9

(d) T_{zeroPR}^{rel}

N	T_{down} 5	15	30	60
2	2.2	1.7	1.7	1.8
3	4.0	3.0	2.6	2.5
10	32.8	14.8	9.0	7.8
15	59.4	23.9	13.9	11.5

(e) $V(WIP)$

N	T_{down} 5	15	30	60
2	74	156	314	630
3	130	270	466	900
10	1004	1332	1632	2790
15	1802	2158	2502	4140

(f) $V(PR)$

N	T_{down} 5	15	30	60
2	16	8	8	8
3	30	22	22	8
10	296	288	288	8
15	666	658	588	8

5.4 Analytical characterization

To obtain an analytical expression for the settling time under FBFS dispatch, we first derive such an expression for the uniform machine allocation and then modify it for the FBFS case. Within the uniform allocation, an equal number of machines is assigned to process lots from each buffer (assuming, for simplicity, that the number of available machines is divisible by N). For this allocation, under condition (3.6), the re-entrant line has steady state (3.5), as it does under FBFS and LBFS. Moreover, this equilibrium is globally attractive, and the transients are of finite duration. Assume that the number of machines operational during the downtime is $M' < Nr$, so that the transients are initiated by downtime-based initial conditions. Then, we have the following:

Theorem 5.2 *The settling time in the re-entrant line (i)-(vii) with $\tau_i = \tau$, $i = 1, 2, \ldots, N-1$, $\tau_0 = \tau_N = 0$ under the uniform allocation and downtime-based initial conditions (5.2) is given by*

$$T_s^{uni} = \left\lceil \frac{\rho - \alpha}{1 - \rho} T_{down} \right\rceil + (N-1)(\tau + 1), \tag{5.6}$$

where $\lceil x \rceil$ is the smallest integer greater than or equal to x and ρ and α are, respectively, the BNWC utilization and the fraction of machines that are up during T_{down}, i.e.,

$$\rho = \frac{Nr}{M}, \ \alpha = \frac{M'}{M}. \tag{5.7}$$

Based on (5.6) and (5.7) and extensive numerical experimentation, we arrived at the following expression for the settling time T_s under FBFS dispatch:

$$T_s^{FBFS} = \begin{cases} \left\lceil \frac{\rho-\alpha}{1-\rho} T_{down} \right\rceil, & \text{if } \frac{\rho}{N(1-\rho)} T_{down} \geqslant \tau + 1, \\ \left\lceil \left(\left\lfloor \frac{\alpha N}{\rho} \right\rfloor + 1 - \frac{\alpha N}{\rho} \right) \frac{\rho}{N(1-\rho)} T_{down} \right\rceil + \left(N - 1 - \left\lfloor \frac{\alpha N}{\rho} \right\rfloor \right)(\tau + 1), & \text{if } \frac{\rho}{N(1-\rho)} T_{down} < \tau + 1, \end{cases} \tag{5.8}$$

where $\lfloor x \rfloor$ is the greatest integer less than or equal to x, and ρ and α are given in (5.7). It turns out that this expression provides a faithful characterization of the settling time in systems at hand. To justify this, we considered a total of 576 re-entrant lines with the parameters selected as all possible combinations of the following sets:

$$N \in \{10, 11, 12, 13, 14, 15\},\ \tau \in \{29, 59, 89\},\ r \in \{1, 2, 3, 4\},$$
$$\kappa \in \{\frac{1}{30}, \frac{1}{15}, \frac{1}{10}, \frac{1}{6}, \frac{1}{5}, \frac{1}{3}, \frac{1}{2}, 1, 2, 3, 4, 5, 6\},$$

where $\kappa = \frac{T_{down}}{\tau+1}$. For 288 of these systems, we have selected $M = 12(r + 1)$, $\alpha \in \{\frac{1}{6}, \frac{1}{4}, \frac{1}{3}, \frac{1}{2}\}$ and for the remaining 288 systems, $\alpha = 0$, $E \in \{1, 2, 3, 4\}$, where, as before, $E = M - Nr$. As a result we obtained:

Numerical Fact 5.1 *For all* 576 *systems analyzed, the settling time evaluated numerically by solving equations (2.12) equals that calculated by (5.8).*

Expression (5.8) can be used to investigate the effects of system parameters on the duration of transients. For instance, consider the following two systems:

$$\begin{aligned} &N = 5,\ M = 52,\ \tau = 29,\ r \in \{6, 7, 8, 9, 10\}, \\ &N = 10,\ M = 52,\ \tau = 29,\ r \in \{3, 4, 5\}. \end{aligned} \tag{5.9}$$

For both of these systems, assume $\alpha \in \{0, 0.25, 0.5\}$, $T_{down} = 15$, and using (5.8), calculate T_s^{FBFS}. The results are shown in Figure 5.4, illustrating to which extend T_s^{FBFS} is increasing in N, decreasing in α, and insensitive to ρ.

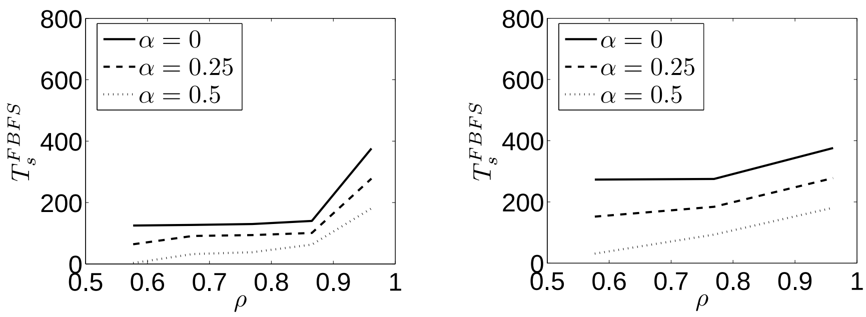

(a) $N = 5$ (b) $N = 10$

Figure 5.4: T_s^{FBFS} as a function of ρ, α, and N

6 Transients under LBFS Dispatch

6.1 Qualitative characterization

Typical trajectories of $WIP(n)$ and $PR(n)$ under LBFS dispatch and downtime-based initial conditions are shown in Tables 6.1-6.3 for the same system as in Subsection 5.2. From these data, we observe:

- Transients of WIP: For $T_{down} \ll \tau$ and small N, the transient response of WIP consists of series of spikes, the number of which equals to N; the spikes in each series are of increasing amplitudes. For all other values of T_{down} and N, the spikes form a "spiked" bubble with the number of spikes in each bubble equal or close to N. The number of bubbles is increasing with T_{down} and N.

- Transients of PR: For all T_{down} and N, the transient response of PR consists of series of pulses, with the amplitudes from $-r$ to $M - r$, centered at PR_{ss}. The series of pulses may be either with monotonically decreasing amplitudes or form a pulsating bubble.

Note that, unlike FBFS, LBFS dispatch always leads to transients with pulsating PR.

Typical transient patterns of $WIP(n)$ and $PR(n)$ are presented in Figures 6.1 and 6.2, respectively, and transients of buffer occupancies of the system with $N = 2$ are shown in Table 6.4.

Table 6.1: Transients under LBFS ($r = 1$)

(a) Transients of $WIP(n)$

N	T_{down} 5	15	30	60
2	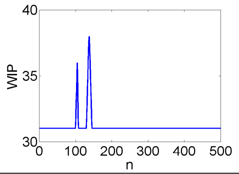	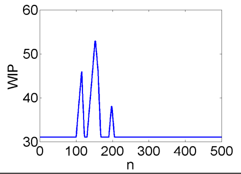	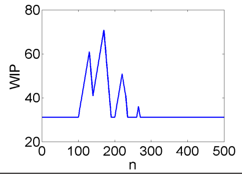	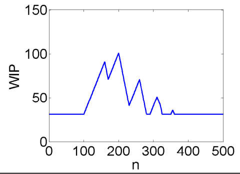
3	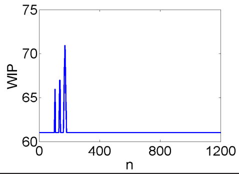	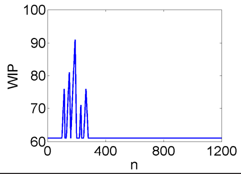	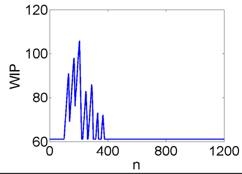	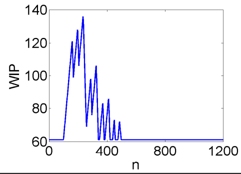
10	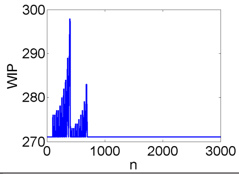	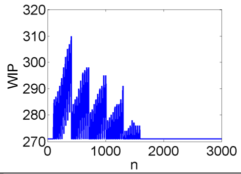	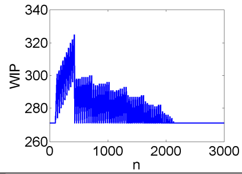	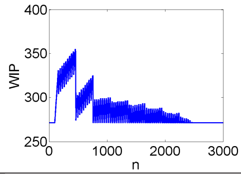
15	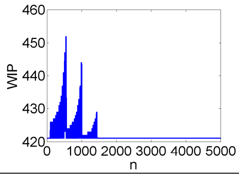	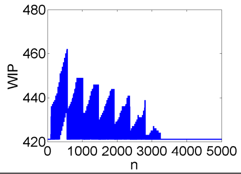	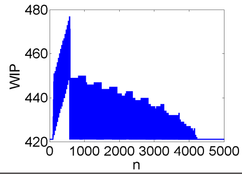	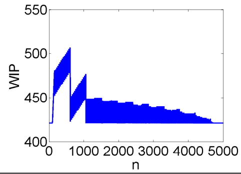

(b) Transients of $PR(n)$

N	T_{down} 5	15	30	60
2	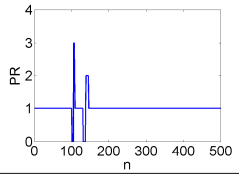	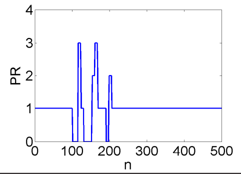	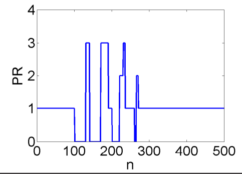	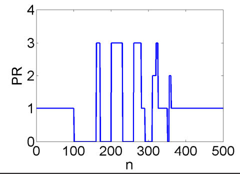
3	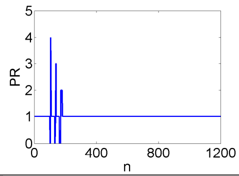	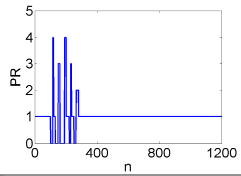	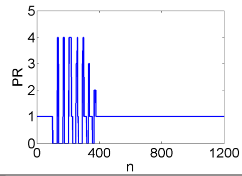	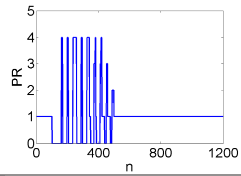
10	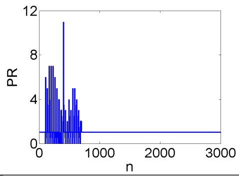	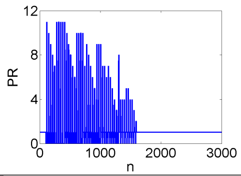	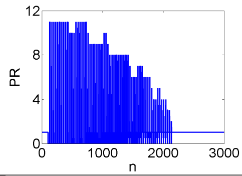	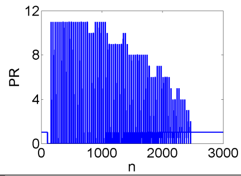
15	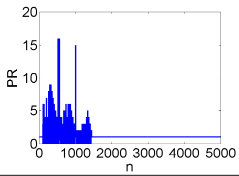	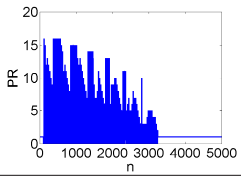	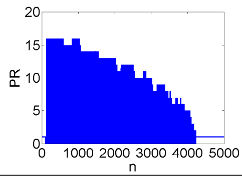	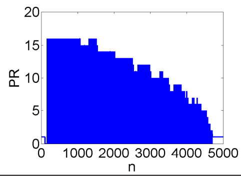

Table 6.2: Transients under LBFS (r = 2)

(a) Transients of $WIP(n)$

<table>
<tr><th rowspan="2">N</th><th colspan="4">T_{down}</th></tr>
<tr><th>5</th><th>15</th><th>30</th><th>60</th></tr>
<tr><td>2</td>
<td>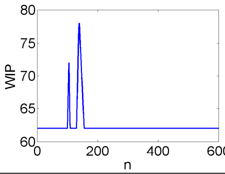
</td>
<td>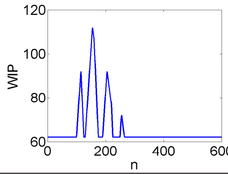
</td>
<td>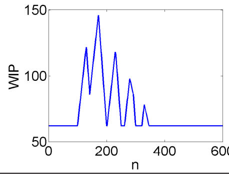
</td>
<td>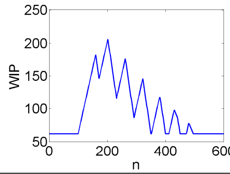
</td></tr>
<tr><td>3</td>
<td>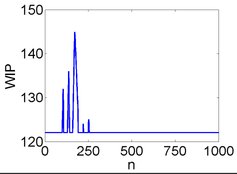
</td>
<td>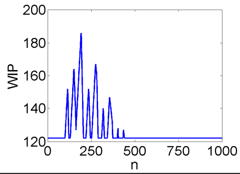
</td>
<td>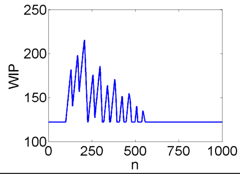
</td>
<td>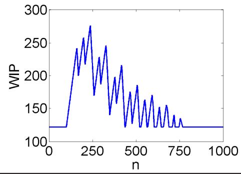
</td></tr>
<tr><td>10</td>
<td>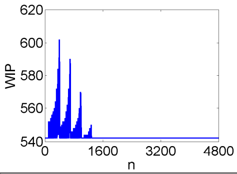
</td>
<td>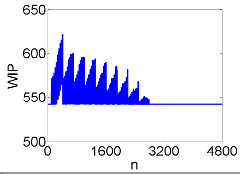
</td>
<td>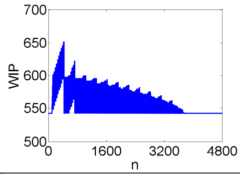
</td>
<td>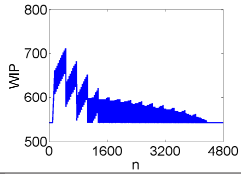
</td></tr>
<tr><td>15</td>
<td>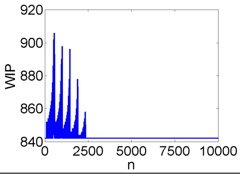
</td>
<td>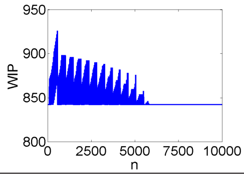
</td>
<td>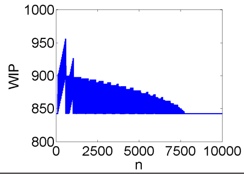
</td>
<td>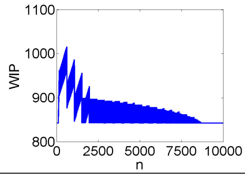
</td></tr>
</table>

(b) Transients of $PR(n)$

<table>
<tr><th rowspan="2">N</th><th colspan="4">T_{down}</th></tr>
<tr><th>5</th><th>15</th><th>30</th><th>60</th></tr>
<tr><td>2</td>
<td>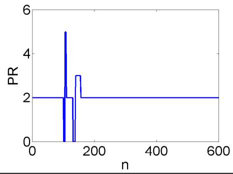
</td>
<td>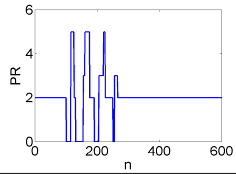
</td>
<td>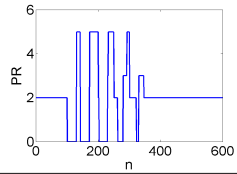
</td>
<td>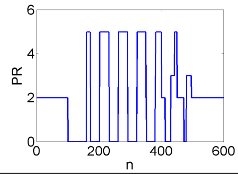
</td></tr>
<tr><td>3</td>
<td>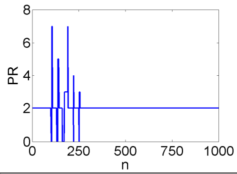
</td>
<td>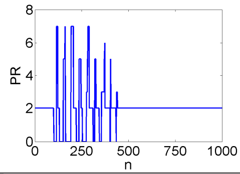
</td>
<td>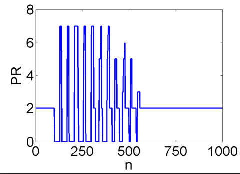
</td>
<td>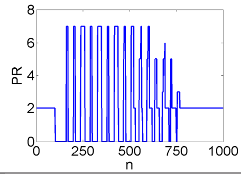
</td></tr>
<tr><td>10</td>
<td>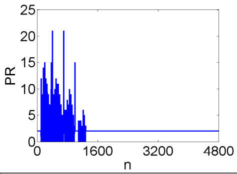
</td>
<td>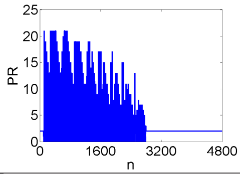
</td>
<td>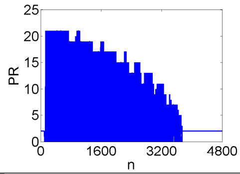
</td>
<td>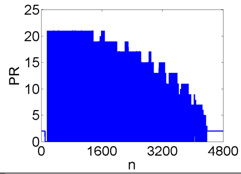
</td></tr>
<tr><td>15</td>
<td>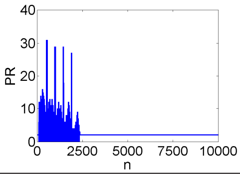
</td>
<td>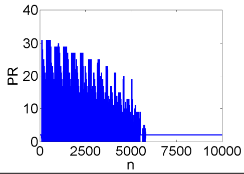
</td>
<td>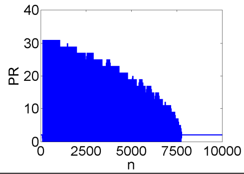
</td>
<td>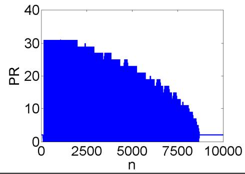
</td></tr>
</table>

Table 6.3: Transients under LBFS (r = 3)

(a) Transients of $WIP(n)$

N	T_{down} 5	15	30	60
2	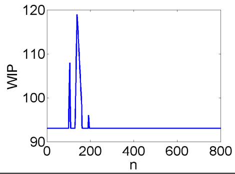	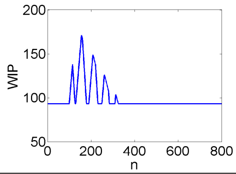	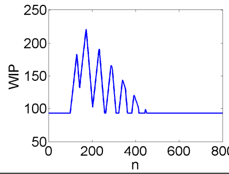	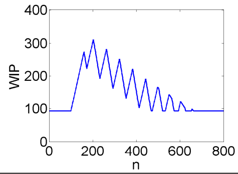
3	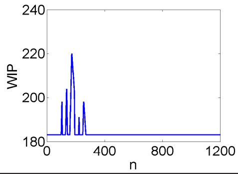	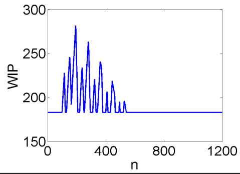	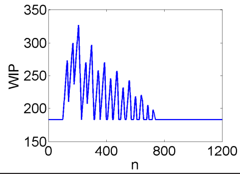	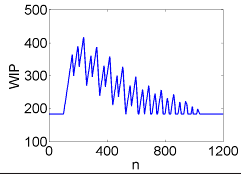
10	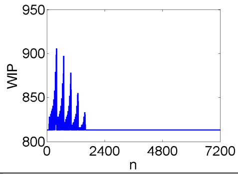	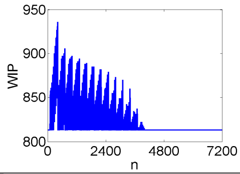	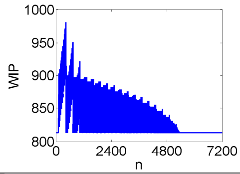	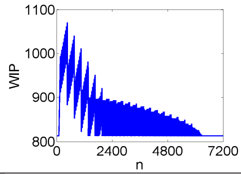
15	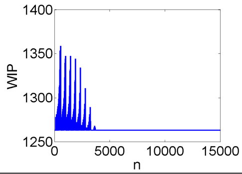	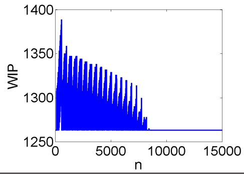	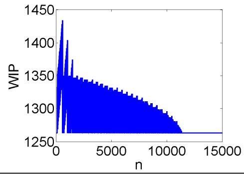	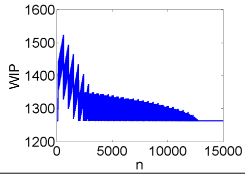

(b) Transients of $PR(n)$

N	T_{down} 5	15	30	60
2	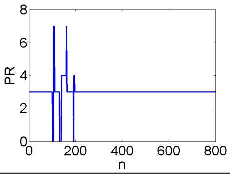	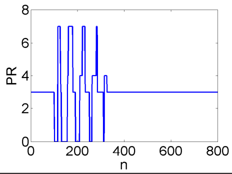	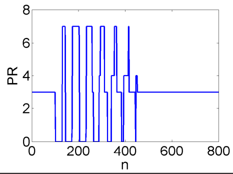	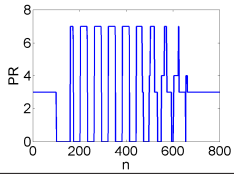
3	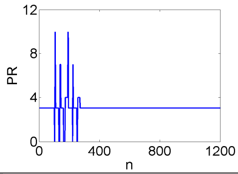	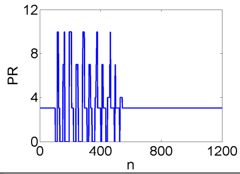	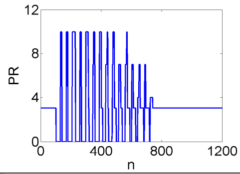	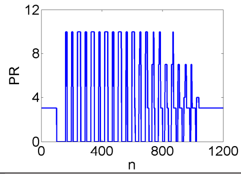
10	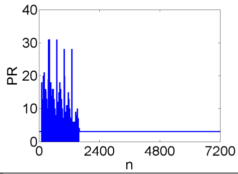	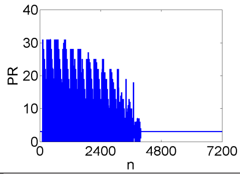	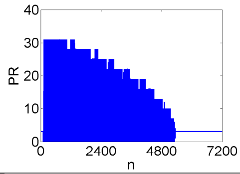	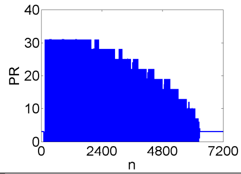
15	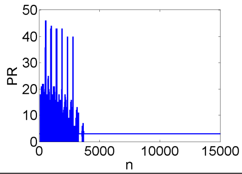	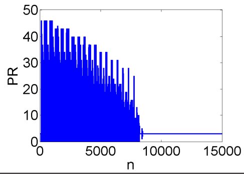	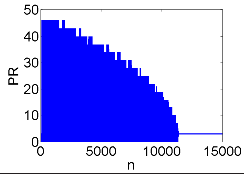	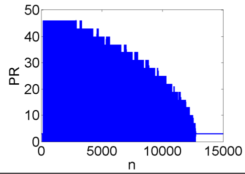

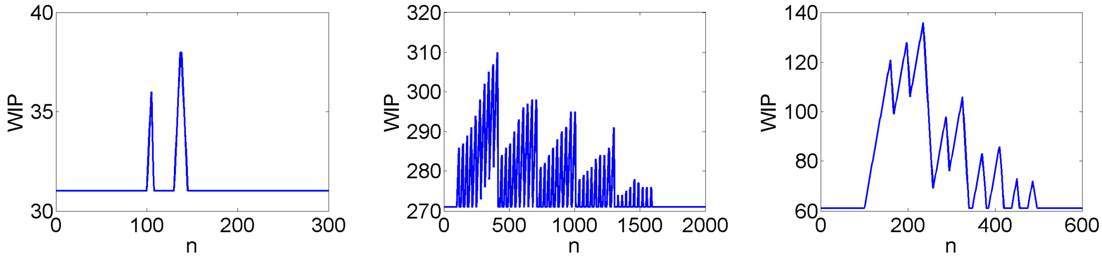

(a) Series of spikes (b) Rippled series of bubbles 1 (c) Rippled series of bubbles 2

Figure 6.1: Typical transient patterns for *WIP*(n) under LBFS

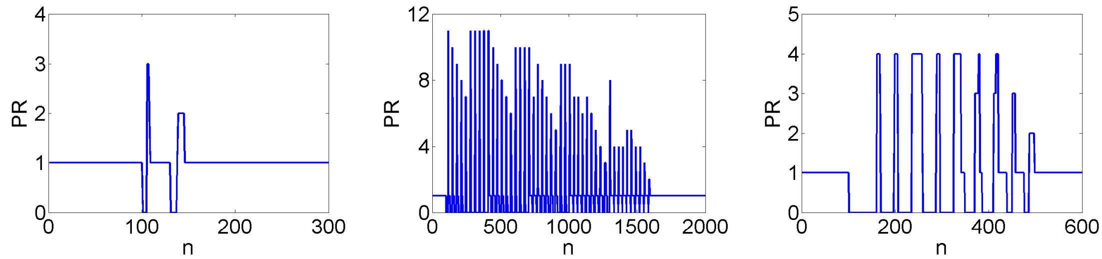

(a) Narrow pulses (b) Rippled series of pulses (c) Decreasing series of pulses

Figure 6.2: Typical transient patterns for *PR*(n) under LBFS

Table 6.4: Transients under LBFS ($N = 2$)

(a) Transients of $x_1(n)$ and $x_2(n)$ ($r = 1$)

x	T_{down}			
	5	15	30	60
x_1	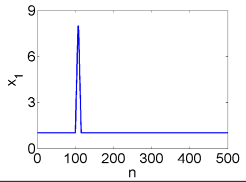	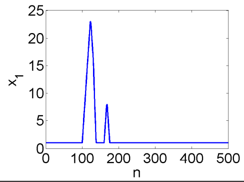	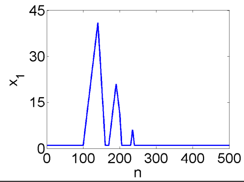	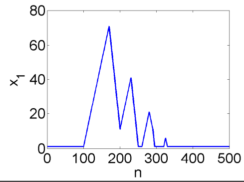
x_2	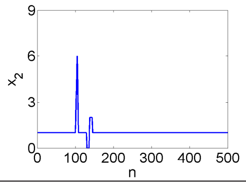	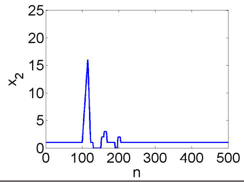	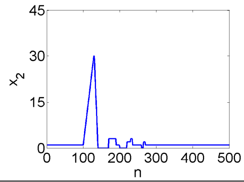	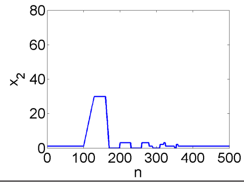

(b) Transients of $x_1(n)$ and $x_2(n)$ ($r = 2$)

x	T_{down}			
	5	15	30	60
x_1	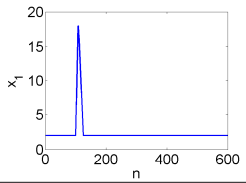	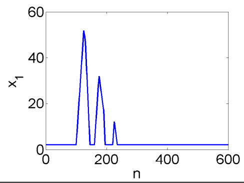	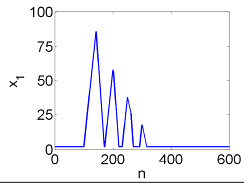	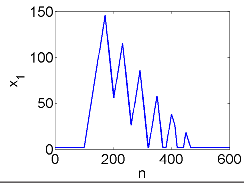
x_2	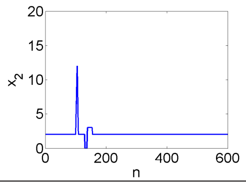	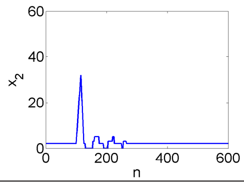	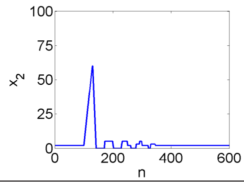	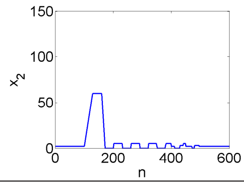

(c) Transients of $x_1(n)$ and $x_2(n)$ ($r = 3$)

x	T_{down}			
	5	15	30	60
x_1	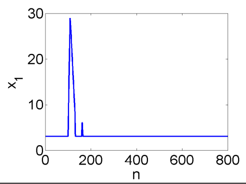	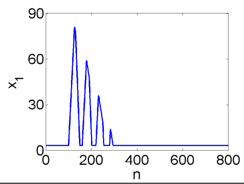	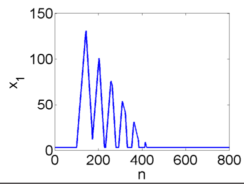	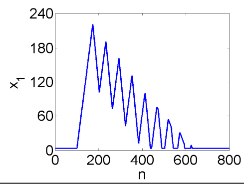
x_2	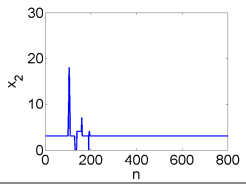	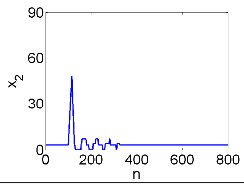	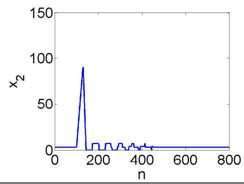	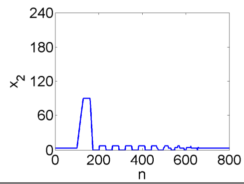

6.2 Empirical quantitative characterization

Using Tables 6.1-6.3, the transient characteristics (2.3)-(2.9) under LBFS are quantified in Tables 6.5-6.7. These tables indicate:

- Relative settling time, T_s^{rel}: Can be as small as 3 and as large as 715; monotonically increasing in N and r and monotonically decreasing in T_{down}.
- Excess of WIP, EX_{WIP}: Can be as small as 0.5% and as large as 85%; monotonically decreasing in N and monotonically increasing in T_{down}.
- Overshoot of RT, OS_{RT}: Can be as small as 7% and as large as 235%; monotonically decreasing in N and monotonically increasing in r and T_{down}.
- Relative zero-PR-time, T_{zeroPR}^{rel}: Can be as small as 2.4 and as large as 272; monotonically increasing in N and r and non-monotonic concave in T_{down}.
- Variability of WIP, $V(WIP)$: Can be as small as 24 and as large as 48800; monotonically increasing in N, r, and T_{down}.
- Variability of PR, $V(PR)$: Can be as small as 10 and as large as 26400; monotonically increasing in N, r, and T_{down}.

Table 6.5: Quantification of transients under LBFS (r = 1)

(a) T_s^{rel}

N	T_{down} = 5	15	30	60
2	8.0	6.0	4.7	3.3
3	15.0	11.0	8.2	5.6
10	118.0	98.4	66.8	38.4
15	266.6	208.2	136.2	75.6

(b) EX_{WIP}

N	T_{down} = 5	15	30	60
2	5.4	20.7	41.7	83.1
3	3.1	12.3	22.1	41.5
10	0.9	2.4	3.7	6.2
15	0.5	1.5	2.3	3.5

(c) OS_{RT}

N	T_{down} = 5	15	30	60
2	22.6	71.0	129.0	225.8
3	16.4	49.2	73.8	123.0
10	10.0	14.4	19.9	31.0
15	7.4	9.7	13.3	20.4

(d) T_{zeroPR}^{rel}

N	T_{down} = 5	15	30	60
2	2.4	2.9	2.8	2.4
3	4.2	6.0	5.3	4.1
10	30.4	48.5	40.7	25.2
15	64.6	103.6	85.0	49.8

(e) $V(WIP)$

N	T_{down} = 5	15	30	60
2	24	88	170	290
3	42	180	318	496
10	304	1456	2442	3024
15	646	3108	5098	5972

(f) $V(PR)$

N	T_{down} = 5	15	30	60
2	10	16	22	28
3	18	32	50	66
10	184	674	1002	1200
15	462	1894	2936	3384

Table 6.6: Quantification of transients under LBFS ($r = 2$)

(a) T_s^{rel}

N	T_{down} 5	15	30	60
2	10.0	10.0	7.2	5.6
3	30.0	21.7	14.2	10.1
10	235.6	178.4	120.2	70.1
15	448.4	379.5	254.0	142.0

(b) EX_{WIP}

N	T_{down} 5	15	30	60
2	7.3	22.0	43.0	85.3
3	2.8	10.5	20.3	39.3
10	0.8	2.3	3.5	5.8
15	0.6	1.4	2.1	3.2

(c) OS_{RT}

N	T_{down} 5	15	30	60
2	25.8	80.6	135.5	232.3
3	19.7	52.5	77.0	126.2
10	11.1	14.8	20.3	31.4
15	7.6	10.0	13.5	20.7

(d) T_{zeroPR}^{rel}

N	T_{down} 5	15	30	60
2	2.6	4.0	3.8	3.4
3	5.0	8.5	7.8	6.4
10	51.4	86.6	72.7	45.6
15	111.6	185.4	155.3	91.7

(e) $V(WIP)$

N	T_{down} 5	15	30	60
2	52	240	456	816
3	104	520	950	1538
10	1030	5216	8738	10954
15	2246	11136	18674	22042

(f) $V(PR)$

N	T_{down} 5	15	30	60
2	16	36	46	66
3	52	104	136	192
10	644	2254	3404	4160
15	1472	6450	10356	12092

Table 6.7: Quantification of transients under LBFS ($r = 3$)

(a) T_s^{rel}

N	T_{down} 5	15	30	60
2	18.0	14.0	10.7	8.4
3	33.0	28.4	20.3	14.7
10	298.8	258.0	173.5	101.8
15	714.6	555.2	374.0	209.5

(b) EX_{WIP}

N	T_{down} 5	15	30	60
2	5.9	22.6	40.3	82.7
3	3.6	11.3	19.9	38.7
10	0.9	2.2	3.4	5.7
15	0.5	1.4	2.1	3.1

(c) OS_{RT}

N	T_{down} 5	15	30	60
2	29.0	83.9	138.7	235.5
3	21.3	54.1	78.7	127.9
10	11.4	15.1	20.7	31.7
15	7.6	10.0	13.5	20.7

(d) T_{zeroPR}^{rel}

N	T_{down} 5	15	30	60
2	2.8	4.9	4.7	4.3
3	6.2	11.3	10.7	8.8
10	69.8	121.4	103.7	65.4
15	159.8	272.5	229.3	135.5

(e) $V(WIP)$

N	T_{down} 5	15	30	60
2	88	446	852	1566
3	192	1022	1932	3192
10	2118	10994	18700	23578
15	4826	24574	41364	48858

(f) $V(PR)$

N	T_{down} 5	15	30	60
2	36	64	92	134
3	76	184	264	384
10	1268	4704	7140	8814
15	3270	13930	22598	26462

6.3 Analytical characterization

Consider the re-entrant line defined by assumptions (i)-(vii) with $\tau_i = \tau$, $i = 1, 2, \ldots, N-1$, $\tau_0 = \tau_N = 0$, LBFS dispatch, the release satisfying (3.6), and assume, as before, that $M' < Nr$. Let T_{s1}^{LBFS} represent the part of T_s^{LBFS} necessary to process a lot in all buffers. Then the following balance equation takes place:

$$Nr(T_{down} + T_{s1}^{LBFS}) - M'T_{down} = MT_{s1}^{LBFS}. \tag{6.1}$$

From this equation, we obtain:

$$T_{s1}^{LBFS} = \left\lceil \frac{Nr - M'}{M - Nr} T_{down} \right\rceil = \left\lceil \frac{\rho - \alpha}{1 - \rho} T_{down} \right\rceil . \tag{6.2}$$

where ρ and α are defined in (5.7).

Let T_{s2}^{LBFS} represent the part of T_s^{LBFS} necessary for a lot to traverse the system, excluding the queuing time in buffers $b_1, b_2, \ldots, b_N$. Obviously,

$$T_{s2}^{LBFS} = (N - 1)(\tau + 1). \tag{6.3}$$

Thus, a lower bound on T_s^{LBFS} can be given as the sum of (6.2) and (6.3):

$$T_s^{LBFS} \geqslant \left\lceil \frac{\rho - \alpha}{1 - \rho} T_{down} \right\rceil + (N - 1)(\tau + 1) =: \overline{T}_s^{LBFS}, \tag{6.4}$$

which is exactly the settling time (5.6) for the uniform allocation derived in Subsection 5.4.

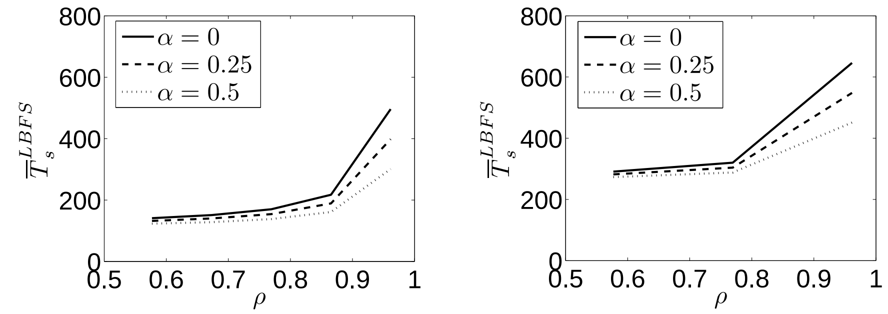

(a) $N = 5$

(b) $N = 10$

Figure 6.3: $\overline{T}_s^{LBFS}$ as a function of ρ, α, and N

The behavior of $\overline{T}_s^{LBFS}$ as a function of ρ, α, and N is illustrated in Figure 6.3 for the systems as in Subsection 5.4.

7 Comparison of Performance under FBFS and LBFS Dispatch

Based on the results of Sections 3-6, the performance of re-entrant lines under FBFS and LBFS can be contrasted as follows:

- **Steady states:** The unique equilibrium of under-loaded systems with FBFS and LBFS are identical and, thus, all steady state performance characteristics are the same. In fully-loaded systems under FBFS, the *WIP* of multiple equilibria contains more lots at the last stage of their processing than under LBFS; the latter, however, contains more lots at the first stage of processing, which is preferable.

- **Stability:** All equilibria of fully-loaded systems are not attractive. The unique equilibrium of under-loaded systems with FBFS dispatch is finite-time globally attractive in the sense that both *WIP* and *PR* return to their steady states within a finite interval of time from any finite initial condition. This is not true for LBFS: for some initial conditions, the system does not return to its equilibrium and locks into either a periodic or a chaotic (bounded aperiodic) regime. Thus, FBFS has a clear advantage from this point of view. Note, however, that if the delays in all re-entrant paths are identical, LBFS also leads to finite-time global stability.

- **Transients:** The conclusions on relative advantages and disadvantages of FBFS and LBFS from the point of view of transients can be derived based on either Tables 5.5-5.7 and 6.5-6.7 or on analytical expressions (5.8) and (6.4). From the latter, it is easy to show that $T_s^{FBFS} \leqslant T_s^{LBFS}$. A more detailed characterization follows from Tables 5.5(a)-5.7(a) and 6.5(a)-6.7(a): T_s^{LBFS} may be up to an order of magnitude longer than T_s^{FBFS}. Similarly, zero-*PR*-time under LBFS may be an order of magnitude longer than under FBFS. Even more dramatic are differences between the variabilities: under LBFS, $V(PR)$ may be up to three orders of magnitude larger than under FBFS. On the other hand, LBFS leads to somewhat smaller EX_{WIP} and OS_{RT}. So, from the transients point of view, each FBFS and LBFS has advantages and disadvantages. However, taking into account that under LBFS the system may not even converge to the equilibrium, one must conclude that the transients induced by FBFS are preferable to those induced by LBFS.

The above arguments lead to the conclusion that, if downtimes in a re-entrant line are common, LBFS dispatch should be avoided as much as possible.

8 Extensions

8.1 Transients for $\tau_i \neq \tau_j$

In Sections 5 and 6, it has been assumed that the delays in all re-entrant paths are the same. Here, we illustrate the system behavior with $\tau_i \neq \tau_j$, while keeping $\tau_0 = \tau_N = 0$.

Consider, for example, one of the systems analyzed in Sections 5 and 6 but with different τ_i's, specifically, the system with

$$N = 3, \ M = 4, \ M' = 0, \tag{8.1}$$

and τ_i's indicated in Tables 8.1 and 8.2. Using equations (2.12), we calculate $WIP(n)$ and $PR(n)$ shown in Tables 8.1 and 8.2 for FBFS and LBFS, respectively. Comparing these data with those of Sections 5 and 6, we observe:

- Different τ_i's do not change the qualitative nature of the transients, as compared with those for identical τ_i's, if the equilibrium for LBFS is attractive; if it is not, the transients are periodic (see the fifth and seventh rows of Tables 8.2(a) and (b)).

- In the quantitative sense, different τ_i's results in relatively insignificant changes as compared with identical τ_i's for FBFS. For LBFS, the changes are more significant but still relatively small.

Table 8.1: Transients under FBFS for non-identical τ's ($N = 3, r = 1$)

(a) Transients of $WIP(n)$

τ_1, τ_2	T_{down}			
	5	15	30	60
19, 29	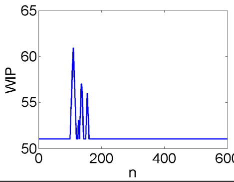	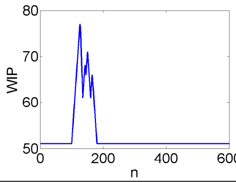	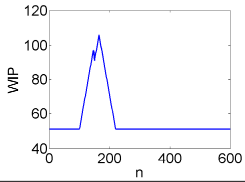	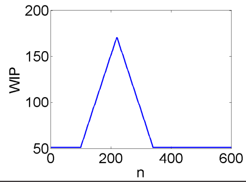
29, 19	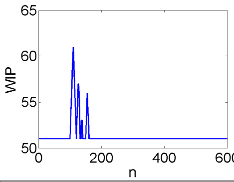	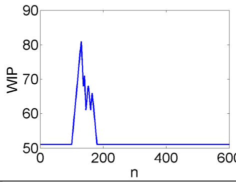	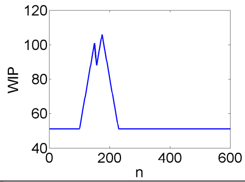	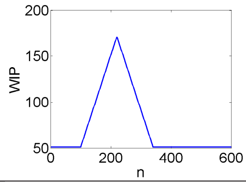
20, 30	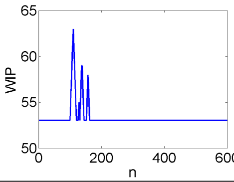	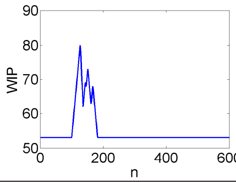	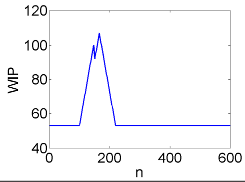	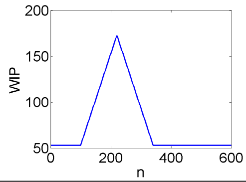
30, 20	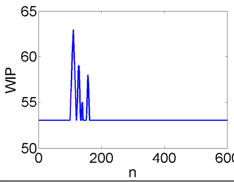	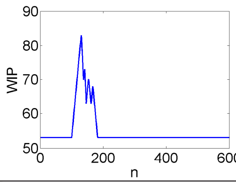	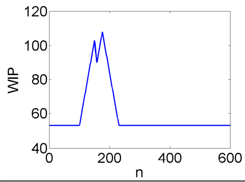	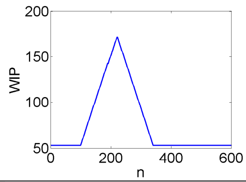
28, 29	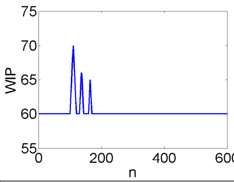	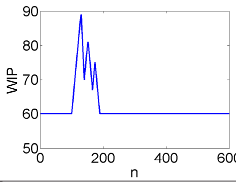	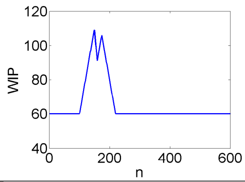	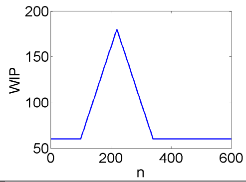
29, 28	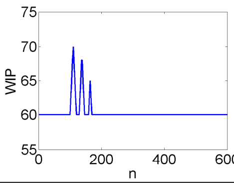	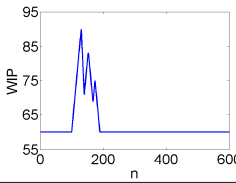	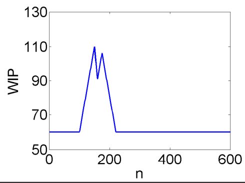	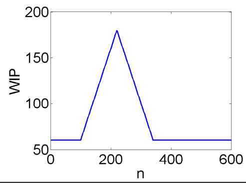
28, 30	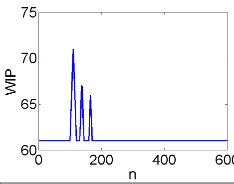	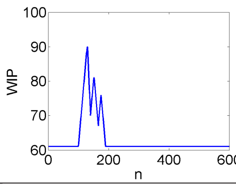	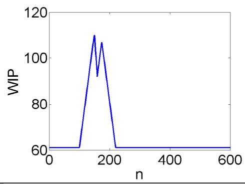	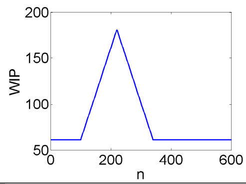
30, 28	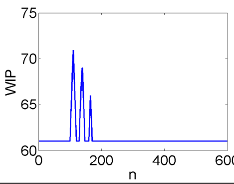	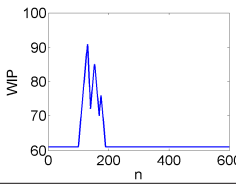	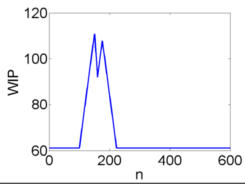	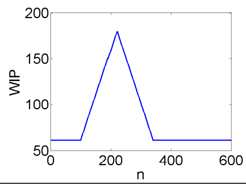

Table 8.1: Transients under FBFS for non-identical τ's ($N = 3, r = 1$) (Cont'd)

(b) Transients of $PR(n)$

τ_1, τ_2	T_{down}			
	5	15	30	60
19, 29	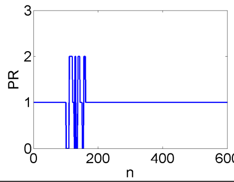	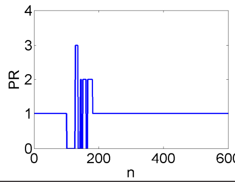	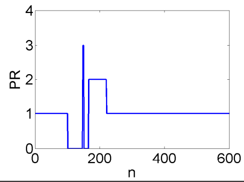	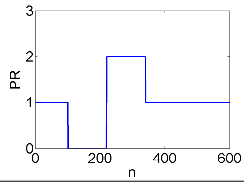
29, 19	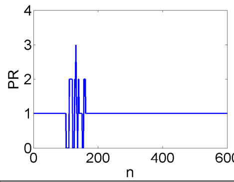	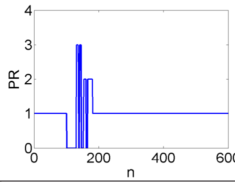	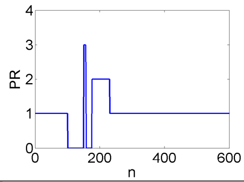	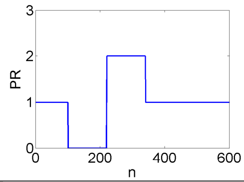
20, 30	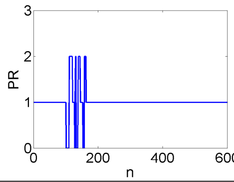	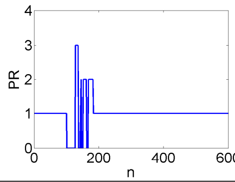	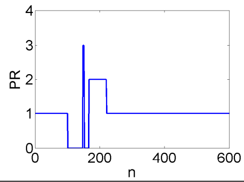	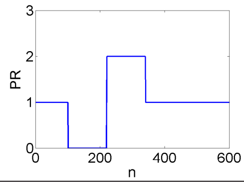
30, 20	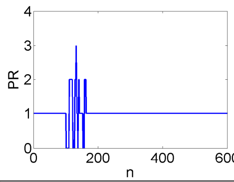	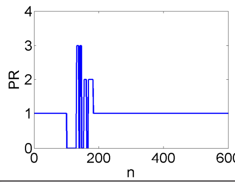	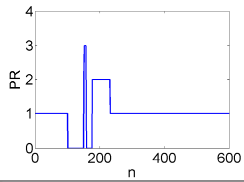	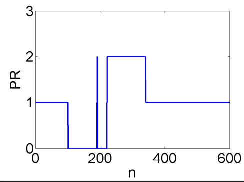
28, 29	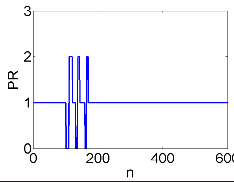	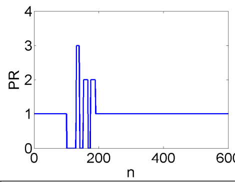	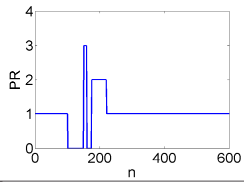	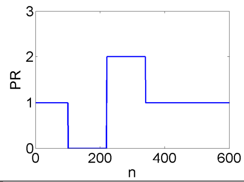
29, 28	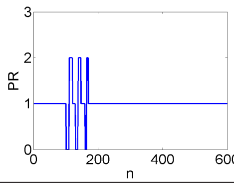	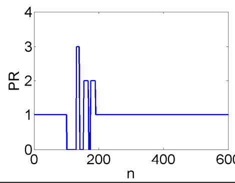	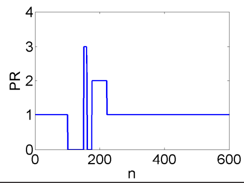	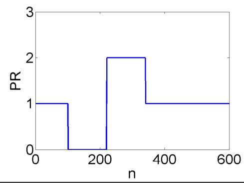
28, 30	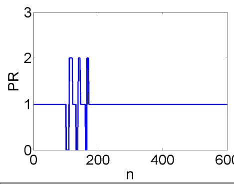	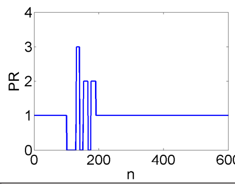	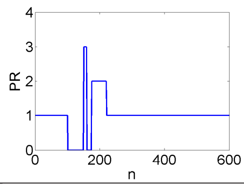	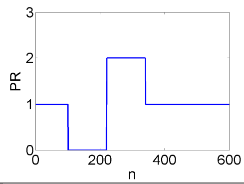
30, 28	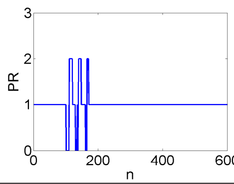	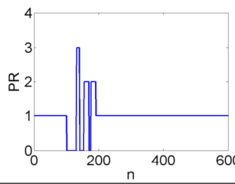	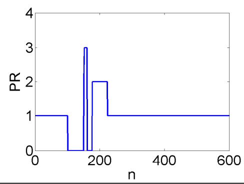	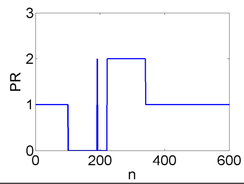

Table 8.2: Transients under LBFS for non-identical τ's ($N = 3, r = 1$)

(a) Transients of *WIP*(n)

τ_1, τ_2	T_{down}			
	5	15	30	60
19, 29	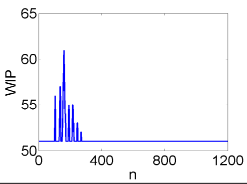	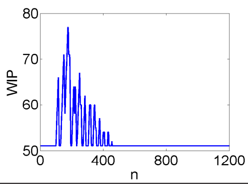	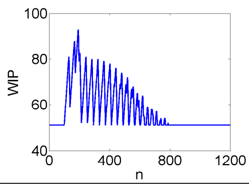	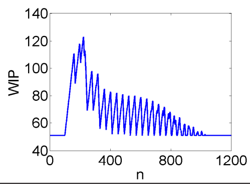
29, 19	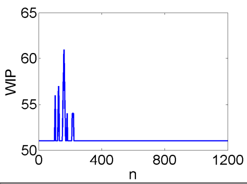	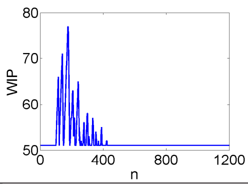	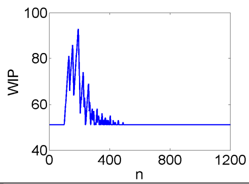	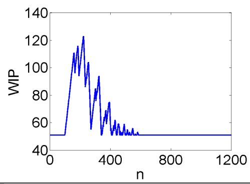
20, 30	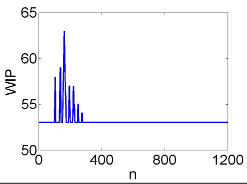	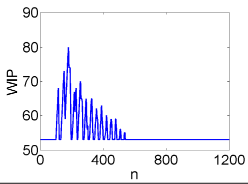	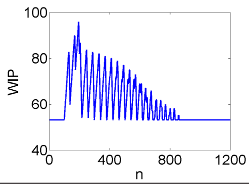	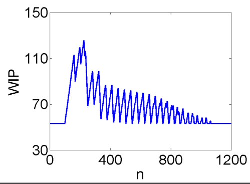
30, 20	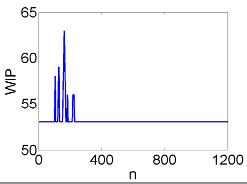	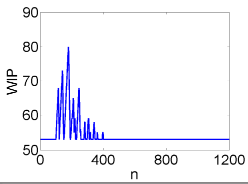	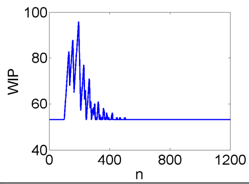	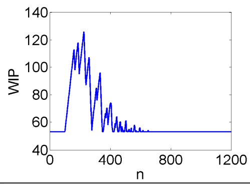
28, 29	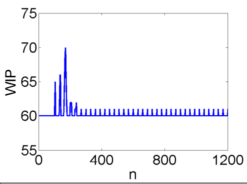	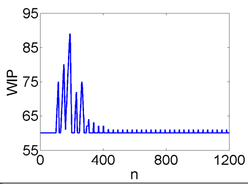	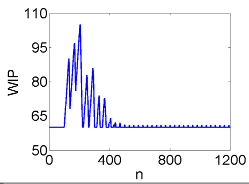	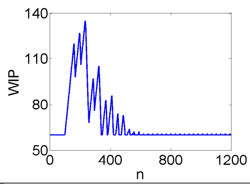
29, 28	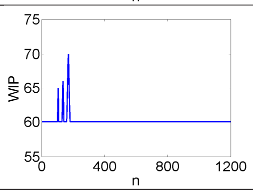	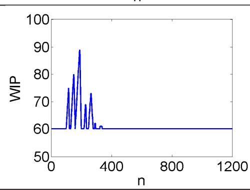	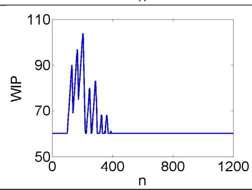	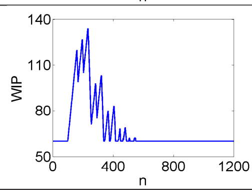
28, 30	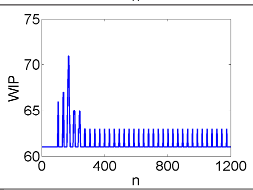	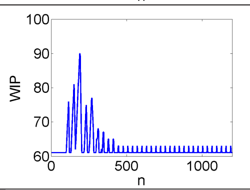	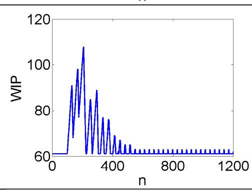	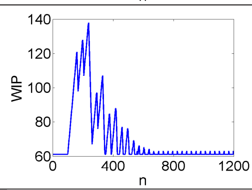
30, 28	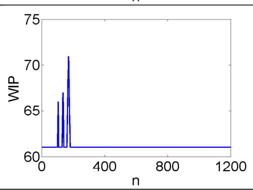	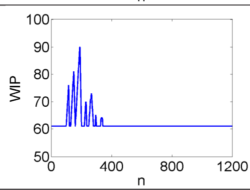	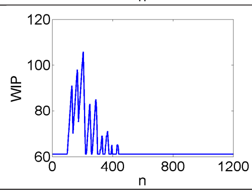	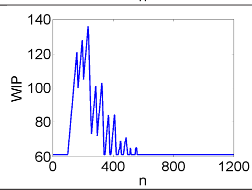

Table 8.2: Transients under LBFS for non-identical τ's ($N = 3, r = 1$) (Cont'd)

(b) Transients of $PR(n)$

τ_1, τ_2	T_{down}			
	5	15	30	60
19, 29	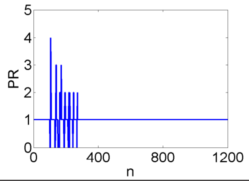	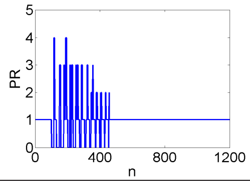	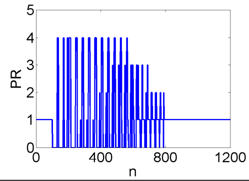	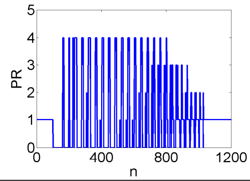
29, 19	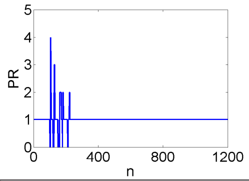	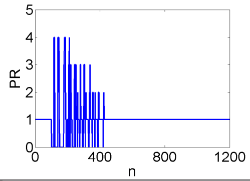	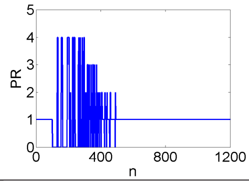	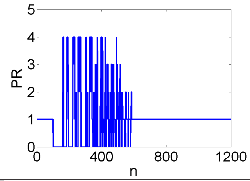
20, 30	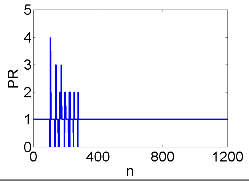	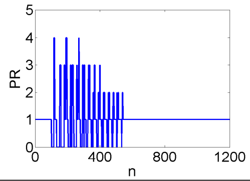	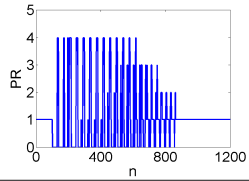	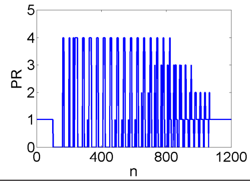
30, 20	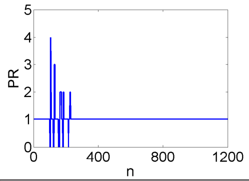	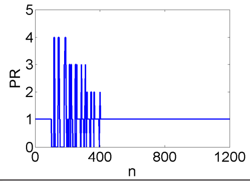	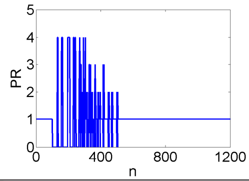	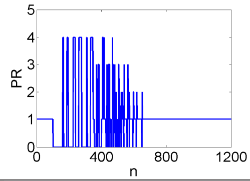
28, 29	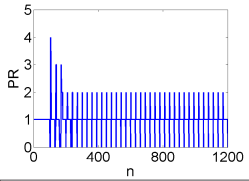	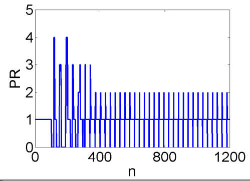	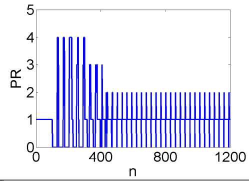	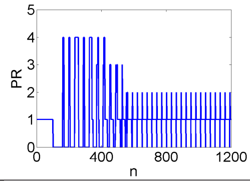
29, 28	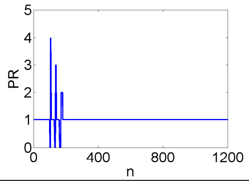	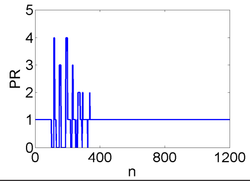	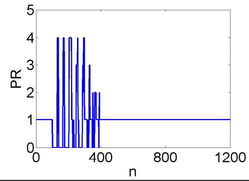	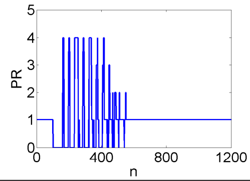
28, 30	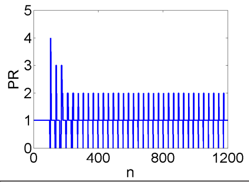	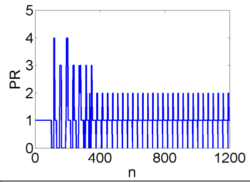	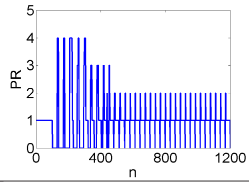	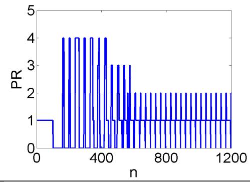
30, 28	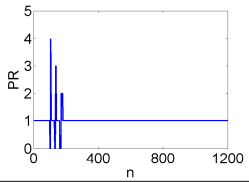	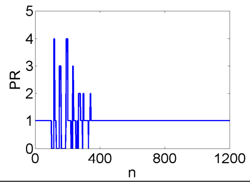	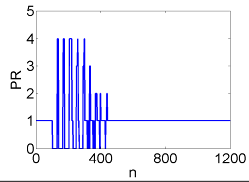	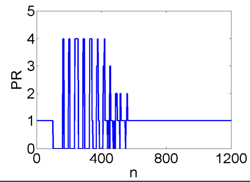

Table 8.3: Quantification of transients under FBFS ($N = 3, r = 1$)

(a) T_s^{rel}

τ_1, τ_2	T_{down} 5	15	30	60
19, 29	11.0	4.3	3.0	3.0
29, 19	11.0	4.3	3.3	3.0
20, 30	11.4	4.5	3.0	3.0
30, 20	11.4	4.5	3.4	3.0
28, 29	12.8	4.9	3.0	3.0
29, 28	12.8	4.9	3.0	3.0
28, 30	13.0	5.0	3.0	3.0
30, 28	13.0	5.0	3.1	3.0

(b) EX_{WIP}

τ_1, τ_2	T_{down} 5	15	30	60
19, 29	5.7	26.1	56.5	117.6
29, 19	5.6	27.5	58.7	117.6
20, 30	5.3	24.9	54.0	113.2
30, 20	5.2	26.6	56.7	112.7
28, 29	4.0	23.0	45.1	100.0
29, 28	4.8	24.3	45.3	100.0
28, 30	3.9	22.0	44.3	98.4
30, 28	4.8	24.5	45.2	98.0

(c) OS_{RT}

τ_1, τ_2	T_{down} 5	15	30	60
19, 29	19.6	51.0	107.8	235.3
29, 19	19.6	58.8	107.8	235.3
20, 30	18.9	50.9	101.9	226.4
30, 20	18.9	56.6	103.8	224.5
28, 29	16.7	48.3	81.7	200.0
29, 28	16.7	50.0	83.3	200.0
28, 30	16.4	47.5	80.3	196.7
30, 28	16.4	49.2	82.0	195.1

(d) T_{zeroPR}^{rel}

τ_1, τ_2	T_{down} 5	15	30	60
19, 29	4.6	2.9	2.0	2.0
29, 19	4.6	3.0	2.3	2.0
20, 30	4.6	2.9	2.1	2.0
30, 20	4.6	3.0	2.3	2.0
28, 29	4.2	3.2	2.1	2.0
29, 28	4.6	3.2	2.2	2.0
28, 30	4.2	3.3	2.1	2.0
30, 28	4.6	3.3	2.2	2.0

(e) $V(WIP)$

τ_1, τ_2	T_{down} 5	15	30	60
19, 29	46	86	122	240
29, 19	46	90	136	240
20, 30	46	88	124	240
30, 20	46	90	136	240
28, 29	42	96	128	240
29, 28	46	96	130	240
28, 30	42	98	128	240
30, 28	46	98	132	240

(f) $V(PR)$

τ_1, τ_2	T_{down} 5	15	30	60
19, 29	16	18	10	4
29, 19	18	20	10	4
20, 30	16	18	10	4
30, 20	18	20	10	8
28, 29	12	14	10	4
29, 28	12	14	10	4
28, 30	12	14	10	4
30, 28	14	14	10	8

Table 8.4: Quantification of transients under LBFS ($N = 3, r = 1$)

(a) T_s^{rel}

τ_1, τ_2	T_{down} 5	15	30	60
19, 29	33.2	22.7	22.0	14.5
29, 19	23.6	20.6	12.0	7.1
20, 30	34.4	28.3	24.4	15.1
30, 20	24.4	19.1	12.5	8.2
28, 29	30*	30*	30*	30*
29, 28	14.8	14.8	8.7	6.5
28, 30	31*	31*	31*	31*
30, 28	15.0	15.1	10.3	6.7

* Period of the system transients in steady state

(b) EX_{WIP}

τ_1, τ_2	T_{down} 5	15	30	60
19, 29	2.4	10.7	22.3	34.9
29, 19	3.0	8.5	16.6	40.8
20, 30	2.3	10.1	21.4	32.9
30, 20	2.8	8.8	15.7	34.7
28, 29	0.1*	0.1*	0.1*	0.1*
29, 28	3.2	9.4	20.5	36.5
28, 30	0.2*	0.2*	0.2*	0.2*
30, 28	3.1	9.3	18.2	35.9

* Measured in one period

(c) OS_{RT}

τ_1, τ_2	T_{down} 5	15	30	60
19, 29	19.6	51.0	82.4	141.2
29, 19	19.6	51.0	82.4	141.2
20, 30	18.9	50.9	81.1	137.7
30, 20	18.9	50.9	81.1	137.7
28, 29	16.7	48.3	75.0	125.0
29, 28	16.7	48.3	73.3	123.3
28, 30	16.4	47.5	77.0	126.2
30, 28	16.4	47.5	73.8	123.0

(d) T_{zeroPR}^{rel}

τ_1, τ_2	T_{down} 5	15	30	60
19, 29	6.6	8.8	12.7	9.3
29, 19	5.4	8.2	5.9	4.5
20, 30	6.6	10.9	13.8	9.4
30, 20	5.4	7.7	5.7	4.5
28, 29	0.03*	0.03*	0.03*	0.03*
29, 28	4.2	5.9	4.9	4.0
28, 30	0.06*	0.06*	0.06*	0.06*
30, 28	4.2	6.2	5.4	4.2

* Measured in one period

(e) $V(WIP)$

τ_1, τ_2	T_{down} 5	15	30	60
19, 29	66	264	762	1110
29, 19	54	246	354	542
20, 30	66	328	830	1130
30, 20	54	232	344	544
28, 29	2*	2*	2*	2*
29, 28	42	178	296	474
28, 30	4*	4*	4*	4*
30, 28	42	186	324	502

* Measured in one period

(f) $V(PR)$

τ_1, τ_2	T_{down} 5	15	30	60
19, 29	42	88	196	242
29, 19	26	98	174	194
20, 30	42	136	204	238
30, 20	26	80	164	172
28, 29	4*	4*	4*	4*
29, 28	18	42	68	92
28, 30	4*	4*	4*	4*
30, 28	18	46	68	84

* Measured in one period

8.2 Transients for nonzero τ_0 and τ_N

In Sections 5 and 6, it has been assumed, for simplicity, that the delays in the input and output paths of model (i)-(vii) are zero. It turns out that the results obtained are easy to generalize for the case $\tau_0 > 0$ and $\tau_N > 0$.

Indeed, equip the notations for the performance measures (2.3)-(2.9) with arguments indicating the values of the delays in input and output paths. Then, we have the following proposition:

Proposition 8.1 *Assume the re-entrant lines defined by assumptions (i)-(vii) have been operating in steady state when they break down for T_{down} time slots. The performance measures (2.3)-(2.9) of a re-entrant line with general τ_0 and τ_N are related to those of a line with $\tau_0 = 0$ and $\tau_N = 0$ as follows:*

$$\begin{aligned}
WIP(n;\tau_0,\tau_N) &= WIP(n-\tau_N;0,0) + (\tau_0+\tau_N)r,\ \forall n \geqslant \tau_N;\\
PR(n;\tau_0,\tau_N) &= PR(n-\tau_N;0,0),\ \forall n \geqslant \tau_N;\\
T_s(\tau_0,\tau_N) &= T_s(0,0) + \tau_N;\\
EX_{WIP}(\tau_0,\tau_N) &\leqslant EX_{WIP}(0,0);\\
OS_{RT}(\tau_0,\tau_N) &\leqslant OS_{RT}(0,0);\\
T_{zeroPR}(\tau_0,\tau_N) &= T_{zeroPR}(0,0);\\
V(WIP;\tau_0,\tau_N) &= V(WIP;0,0);\\
V(PR;\tau_0,\tau_N) &= V(PR;0,0).
\end{aligned} \tag{8.2}$$

8.3 Transients in re-entrant line models with multiple workcenters

The purpose of this subsection is to illustrate that systems with multiple workcenters behave similarly (or even identically) to their BNWC-based models. To accomplish this, consider the re-entrant line with three workcenters shown in Figure 8.1. Assume that

$$M_1 = 8,\ M_2 = 7,\ M_3 = 8,\ N = 3,\ r = 2, \tag{8.3}$$

where M_i is the number of machines in the i-th workcenter. Thus, the second workcenter has the highest utilization, $\rho_2 = \frac{Nr}{M_2} = 0.86$ and, thus, is the bottleneck. Along with this, consider the BNWC-based model of this system (Figure 1.1), which, according to (8.3), has the following parameters:

$$M = 7,\ N = 3,\ \tau_0 = 1,\ \tau_1 = 2,\ \tau_2 = 2,\ \tau_3 = 1,\ r = 2. \tag{8.4}$$

To compare the performance of these two systems, we have constructed the finite-difference equations that describe the system of Figure 8.1 and solved them numerically, along with equations (2.12) that describe the system of Figure 1.1. For both systems, the initial conditions were downtime-based, and the downtime of duration 5 slots commenced at $n = 11$. The results are given in Figures 8.2 and 8.3 for FBFS and for LBFS, respectively. As one can see, the trajectories of $WIP(n)$ and $PR(n)$ in both cases are identical. Thus, in this example, the BNWC-based model provides a faithful description of the original system. A detailed analysis of this phenomenon is a topic of future work.

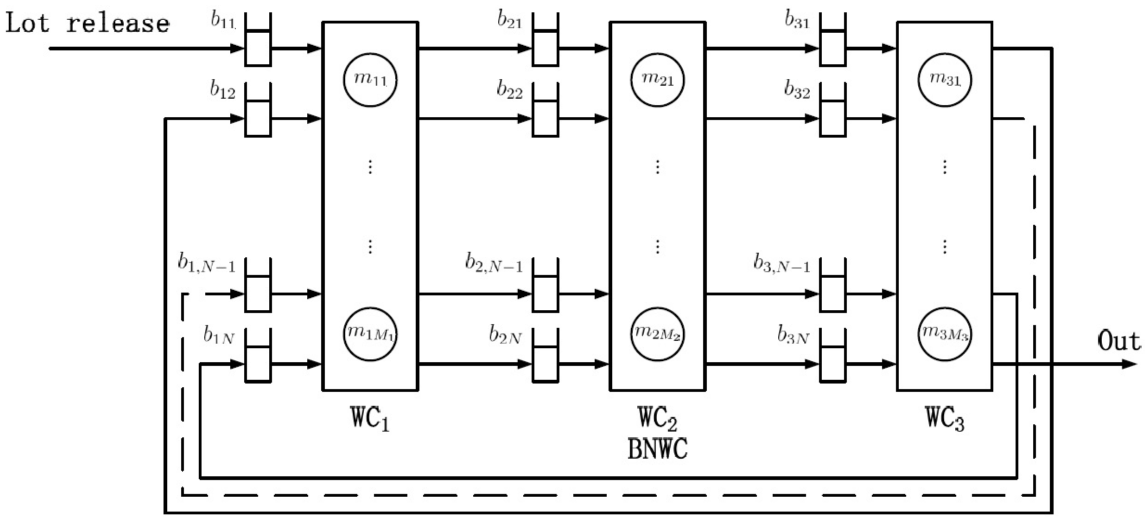

Figure 8.1: Re-entrant line with 3 workcenters

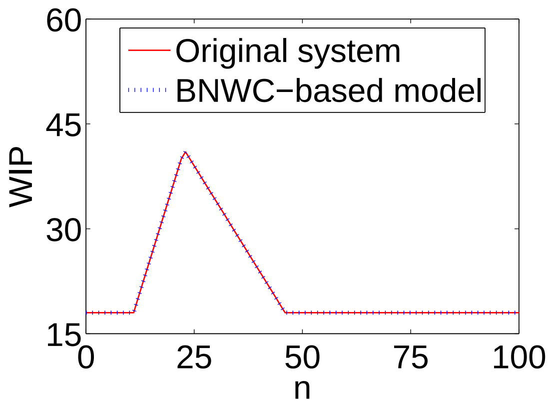

(a) Comparison of *WIP*

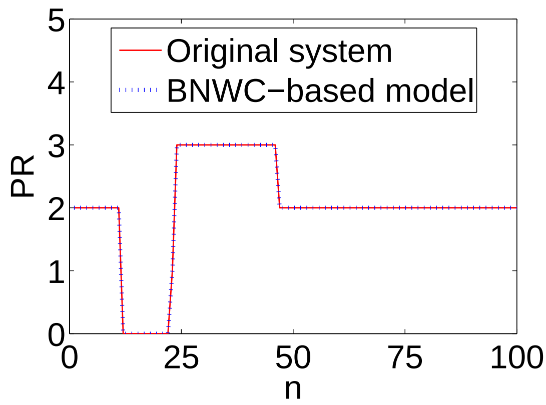

(b) Comparison of *PR*

Figure 8.2: Comparison of 3-workcenter model and BNWC-based model under FBFS dispatch

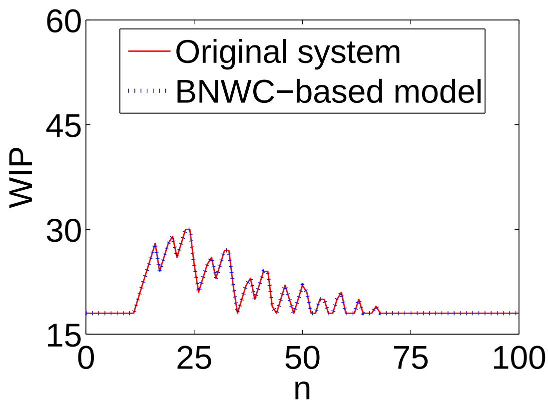

(a) Comparison of *WIP*

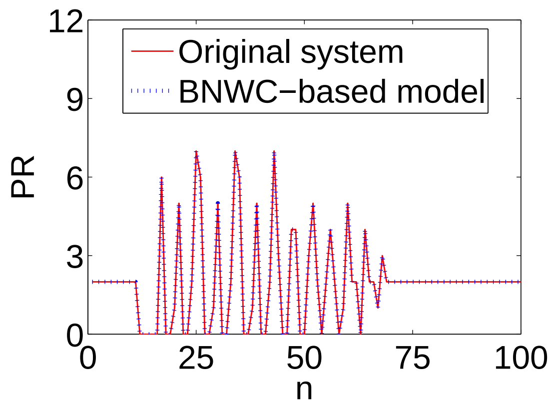

(b) Comparison of *PR*

Figure 8.3: Comparison of 3-workcenter model and BNWC-based model under LBFS dispatch

9 Conclusions and Future Work

This paper analyzed re-entrant lines using the methods of nonlinear dynamics. It demonstrated that re-entrant lines exhibit rich patterns of dynamic behavior and investigated some, but by no means all, of them. First, only the simplest, bottleneck workcenter-based model has been analyzed. Second, only two dispatch policies, FBFS and LBFS, have been considered. Third, only constant lot release policy is discussed.

Under this scenario, the main conclusion is that LBFS dispatch has poor dynamic response to machine downtime, leading to long transients, high *WIP* and *PR* variability, and long intervals of zero-*PR*. From all these points of view, FBFS exhibits a better performance but still suffers from pulsating *WIP* and *PR*. So, how can the dynamics of re-entrant lines be improved? The answer is, perhaps, in introducing feedback control of lot release. In terms of the model considered here, this would imply that r should be a function of either the machine status (machine-based feedback) or the buffer occupancy (buffer-based feedback). Note that, using simulations, feedback release has been analyzed in numerous publications (see, for instance, [28]-[34]) but no analytical results have been obtained. We plan to investigate this issue in future work.

Also, the future work will include: dispatch policies other than FBFS and LBFS; machines with different cycle time; multi-product systems; finite buffers; re-entrant lines with random machine downtime; a more complete study of systems with multiple workcenters and, perhaps, multiple bottlenecks; application of results obtained to practical systems for the purposes of analysis, design, and continues improvement.

From the theoretical perspective, future research will include the development of specialized methods for analysis of nonlinear equations of the type (2.12) and detailed investigation of chaotic regimes illustrated in Figure 4.4(c).

Acknowledgement

The authors are grateful to the University of Michigan undergraduate student J. Zhou for his work on justification of Numerical Fact 5.1. The authors acknowledge also financial support of the National Science Foundation under the Grant No. 0758259 and China Scholarship Council (CSC).

Appendix

Proof of Theorem 3.1: First, we prove the theorem for buffer-based priority dispatch policies and then comment on the general case.

Assume (2.12) has a steady state. Then, from the first three equations of (2.12), we obtain:

$$v_1(x_1^{ss}, x_2^{ss}, \ldots, x_N^{ss}) = z_{0,\tau_0}^{ss} = \ldots = z_{01}^{ss} = r. \tag{A.1}$$

Similarly, from the next three equations and the last two equations of (2.12), respectively, we have

$$v_i(x_1^{ss}, x_2^{ss}, \dots, x_N^{ss}) = z_{i-1,\tau_{i-1}}^{ss} = \dots = z_{i-1,1}^{ss} = v_{i-1}(x_1^{ss}, x_2^{ss}, \dots, x_N^{ss}),\ i = 2, 3, \dots, N, \tag{A.2}$$

$$z_{N,\tau_N}^{ss} = \dots = z_{N1}^{ss} = v_N(x_1^{ss}, x_2^{ss}, \dots, x_N^{ss}). \tag{A.3}$$

Thus, from (A.1)-(A.3),

$$\boldsymbol{z}_i^{ss} = [z_{i1}^{ss} = r, z_{i2}^{ss} = r, \dots, z_{i,\tau_i}^{ss} = r]^T,\ i = 0, 1, \dots, N, \tag{A.4}$$

$$v_i(x_1^{ss}, x_2^{ss}, \dots, x_N^{ss}) = r,\ i = 1, 2, \dots, N. \tag{A.5}$$

Since (A.5) implies $M \geqslant Nr$, it follows that a steady state exists only if (3.3) is satisfied.

The case of general dispatch policies is proved similarly by replacing $v_i(x_1^{ss}, x_2^{ss}, \dots, x_N^{ss})$ with $\min\{v_i(x_1^{ss}, x_2^{ss}, \dots, x_N^{ss}), x_i^{ss}\}$ in the proof (note that in this case, the difference equations is (2.2)). ■

Proof of Theorem 3.2: We prove this theorem for FBFS dispatch. The case of LBFS is proved similarly.

When the system is in the steady state, as it is shown in the proof of Theorem 3.1, $v_i(x_1^{ss}, x_2^{ss}, \dots, x_N^{ss}) = r$, $i = 1, 2, \dots, N$, therefore, from the definition of S_i, we have

$$S_i = (i-1)r,\ i = 1, 2, \dots, N.$$

When $r \leqslant \frac{M}{N}$, $M - S_i \geqslant (N - i + 1)r$, $i = 1, 2, \dots, N$, which implies that $M - S_i > r$, $\forall i \in \{1, 2, \dots, N-1\}$ and $M - S_N > r$ if and only if $r < \frac{M}{N}$ and $M - S_N = r$ if and only if $r = \frac{M}{N}$. Thus, taking into account (2.10) and $v_i(x_1^{ss}, x_2^{ss}, \dots, x_N^{ss}) = r$, $i = 1, 2, \dots, N$, we obtain:

$$\boldsymbol{x}^{ss} = [x_1^{ss} = r, x_2^{ss} = r, \dots, x_N^{ss} = r]^T,\ \text{if and only if } r < \frac{M}{N},$$

$$\boldsymbol{x}^{ss} = [x_1^{ss} = r, x_2^{ss} = r, \dots, x_N^{ss} = q]^T,\ q \geqslant r,\ \text{if and only if } r = \frac{M}{N}.$$

■

To prove Theorems 4.1 and 4.2, we represent equations (2.12) in vector-matrix notations:

$$\boldsymbol{X}(n+1) = \boldsymbol{A}\boldsymbol{X}(n) + \boldsymbol{B}\boldsymbol{u}(n), \tag{A.6}$$

where $\boldsymbol{X}(n) = [(\boldsymbol{x}(n))^T, (\boldsymbol{z_0}(n))^T, (\boldsymbol{z_1}(n))^T, \ldots, (\boldsymbol{z_N}(n))^T]^T$, $\boldsymbol{x}(n) = [x_1(n), x_2(n), \ldots, x_N(n)]^T$, $\boldsymbol{z_i}(n) = [z_{i1}(n), z_{i2}(n), \ldots, z_{i,\tau_i}(n)]^T$, $i = 0, 1, \ldots, N$, $\boldsymbol{u}(n) = [M'(n), r]^T$, and $\boldsymbol{A} \in \mathbb{R}^{(N+\sum_{i=0}^{N}\tau_i)\times(N+\sum_{i=0}^{N}\tau_i)}$ and $\boldsymbol{B} \in \mathbb{R}^{(N+\sum_{i=0}^{N}\tau_i)\times 2}$ are matrices that can be partitioned as follows:

$$\boldsymbol{A} = \begin{bmatrix} (\boldsymbol{A_{11}})_{N\times N} & (\boldsymbol{A_{12}})_{N\times\tau_0} & (\boldsymbol{A_{13}})_{N\times\tau_1} & \cdots & (\boldsymbol{A_{1,N+2}})_{N\times\tau_N} \\ (\boldsymbol{A_{21}})_{\tau_0\times N} & (\boldsymbol{A_{22}})_{\tau_0\times\tau_0} & (\boldsymbol{A_{23}})_{\tau_0\times\tau_1} & \cdots & (\boldsymbol{A_{2,N+2}})_{\tau_0\times\tau_N} \\ (\boldsymbol{A_{31}})_{\tau_1\times N} & (\boldsymbol{A_{32}})_{\tau_1\times\tau_0} & (\boldsymbol{A_{33}})_{\tau_1\times\tau_1} & \cdots & (\boldsymbol{A_{3,N+2}})_{\tau_1\times\tau_N} \\ \vdots & \vdots & \vdots & \ddots & \vdots \\ (\boldsymbol{A_{N+2,1}})_{\tau_N\times N} & (\boldsymbol{A_{N+2,2}})_{\tau_N\times\tau_0} & (\boldsymbol{A_{N+2,3}})_{\tau_N\times\tau_1} & \cdots & (\boldsymbol{A_{N+2,N+2}})_{\tau_N\times\tau_N} \end{bmatrix}, \boldsymbol{B} = \begin{bmatrix} (\boldsymbol{B_1})_{N\times 2} \\ (\boldsymbol{B_2})_{\tau_0\times 2} \\ (\boldsymbol{B_3})_{\tau_1\times 2} \\ \vdots \\ (\boldsymbol{B_{N+2}})_{\tau_N\times 2} \end{bmatrix}. \tag{A.7}$$

To characterize matrices $\boldsymbol{A}$ and $\boldsymbol{B}$ for the case of $\tau_i \neq 0$, $\forall i = 0, 1, \ldots, N$, first we define the submatrices $\boldsymbol{A_{ij}}$ and $\boldsymbol{B_i}$, which are independent of the dispatch policy and linearity region, and then the remaining ones. Those that are independent are:

$$\boldsymbol{A_{21}} = \boldsymbol{0};$$

$$\boldsymbol{A_{1,N+2}} = \boldsymbol{0};$$

$$(\boldsymbol{A_{1j}})_{kl} = \begin{cases} 1, & \text{if } k = j-1, l = \tau_{k-1}, \\ 0, & \text{otherwise,} \end{cases}$$

$$2 \leqslant j \leqslant N+1;$$

$$\boldsymbol{A_{ii}} = \begin{bmatrix} \boldsymbol{0}_{1\times(\tau_{i-2}-1)} & 0 \\ \boldsymbol{I}_{\tau_{i-2}-1} & \boldsymbol{0}_{(\tau_{i-2}-1)\times 1} \end{bmatrix},$$

$$2 \leqslant i \leqslant N+2;$$

$$\boldsymbol{A_{ij}} = \mathbf{0},$$

$$i \neq j,\ 2 \leqslant i, j \leqslant N + 2;$$

$$(\boldsymbol{B_2})_{kl} = \begin{cases} 1, & \text{if } k = 1, l = 2, \\ 0, & \text{otherwise.} \end{cases}$$

The submatrices, which depend on the dispatch and linearity region s are: For FBFS:

- $1 \leqslant s \leqslant N$,

$$(\boldsymbol{A_{11}})_{kl} = \begin{cases} 1, & \text{if } s \geqslant 2, k = N + 2 - s, 1 \leqslant l \leqslant k \text{ or } s \geqslant 3, N + 3 - s \leqslant k = l \leqslant N, \\ 0, & \text{otherwise;} \end{cases}$$

$$(\boldsymbol{B_1})_{kl} = \begin{cases} -1, & \text{if } s \geqslant 2, k = N + 2 - s, l = 1, \\ 0, & \text{otherwise.} \end{cases}$$

- $s \leqslant N$ and $3 \leqslant i \leqslant N + 3 - s$,

$$(\boldsymbol{A_{i1}})_{kl} = \begin{cases} 1, & \text{if } k = 1, l = i - 2, \\ 0, & \text{otherwise;} \end{cases}$$

$$\boldsymbol{B_i} = \mathbf{0}.$$

- $s \geqslant 2$ and $i = N + 4 - s$,

$$(\boldsymbol{A_{i1}})_{kl} = \begin{cases} -1, & \text{if } s \leqslant N, k = 1, 1 \leqslant l \leqslant N + 1 - s, \\ 0, & \text{otherwise;} \end{cases}$$

$$(\boldsymbol{B_i})_{kl} = \begin{cases} 1, & \text{if } k = l = 1, \\ 0, & \text{otherwise.} \end{cases}$$

- $s \geqslant 3$ and $N + 5 - s \leqslant i \leqslant N + 2$,

$$\boldsymbol{A}_{i\mathbf{1}} = \mathbf{0};$$

$$\boldsymbol{B}_i = \mathbf{0}.$$

For LBFS:

- $1 \leqslant s \leqslant N + 1$,

$$(\boldsymbol{A}_{\mathbf{11}})_{kl} = \begin{cases} 1, & \text{if } s \geqslant 2, k = s - 1, k \leqslant l \leqslant N \text{ or } s \geqslant 3, 1 \leqslant k = l \leqslant s - 2, \\ 0, & \text{otherwise,} \end{cases}$$

$$(\boldsymbol{B}_{\mathbf{1}})_{kl} = \begin{cases} -1, & \text{if } s \geqslant 2, k = s - 1, l = 1, \\ 0, & \text{otherwise.} \end{cases}$$

- $s \geqslant 3$ and $3 \leqslant i \leqslant s$,

$$\boldsymbol{A}_{i\mathbf{1}} = \mathbf{0};$$

$$\boldsymbol{B}_i = \mathbf{0}.$$

- $s \geqslant 2$ and $i = s + 1$,

$$(\boldsymbol{A}_{i\mathbf{1}})_{kl} = \begin{cases} -1, & \text{if } k = 1, s \leqslant l \leqslant N, \\ 0, & \text{otherwise,} \end{cases}$$

$$(\boldsymbol{B}_i)_{kl} = \begin{cases} 1, & \text{if } k = l = 1, \\ 0, & \text{otherwise.} \end{cases}$$

- $s \leqslant N$ and $s + 2 \leqslant i \leqslant N + 2$,

$$(\boldsymbol{A}_{i\mathbf{1}})_{kl} = \begin{cases} 1, & \text{if } k = 1, l = i - 2, \\ 0, & \text{otherwise;} \end{cases}$$

$$\boldsymbol{B}_i = \mathbf{0}.$$

Now, we consider systems when τ_0 and/or τ_N are 0.

- $\tau_0 = 0$, $\tau_N \neq 0$: Matrix $\boldsymbol{A}$ remains the same as in (A.7) but with the second row and the second column deleted. In matrix $\boldsymbol{B}$, the second row is deleted and $(\boldsymbol{B_1})_{12} = 1$. All other submatrices remain the same.

- $\tau_N = 0$ $\tau_0 \neq 0$: Matrix $\boldsymbol{A}$ remains the same as in (A.7) but with the last row and the last column deleted. In matrix $\boldsymbol{B}$, the last row is deleted. All other submatrices remain the same.

- $\tau_0 = 0$, $\tau_N = 0$: The changes in $\boldsymbol{A}$ and $\boldsymbol{B}$ are the combined changes from the above two cases.

Although matrix $\boldsymbol{A}$ has different forms in all cases considered above, its characteristic polynomial in Region 1 for both FBFS and LBFS and for all τ_i's remains the same and is given by

$$\det(\lambda \boldsymbol{I} - \boldsymbol{A}) = \lambda^{N+\sum_{i=0}^{N}\tau_i}. \tag{A.8}$$

In Region $s = 2, 3, \ldots, N+1$, the characteristic polynomial depends on the dispatch; specifically,

$$\det(\lambda \boldsymbol{I} - \boldsymbol{A}) = (\lambda - 1)^{s-1}\lambda^{N+1-s+\sum_{i=0}^{N}\tau_i} \text{ for FBFS,} \tag{A.9}$$

$$\det(\lambda \boldsymbol{I} - \boldsymbol{A}) = (\lambda - 1)^{s-1}\lambda^{\tau_N+\sum_{i=0}^{s-2}\tau_i}\sum_{i=0}^{N-s+1}\lambda^{i+\sum_{j=N-i}^{N-1}\tau_j} \text{ for LBFS.} \tag{A.10}$$

These characteristic polynomials are the basis for the local stability analysis.

Proof of Theorem 4.1: Since for $s = 2$, there are eigenvalues of (A.9) and (A.10) at $\lambda = 1$, the convergence to the equilibria in Region 2 does not take place for either FBFS or LBFS. ∎

Proof of Theorem 4.2: Equilibrium (3.5) is in the interior of Region 1 under both FBFS and LBFS dispatch and the characteristic polynomial of $\boldsymbol{A}$ is given by (A.8). Since all eigenvalues of $\boldsymbol{A}$ are at $\lambda = 0$, steady state (3.5) is finite-time attractive under both FBFS and LBFS dispatch.

To complete the proof of the stability, we must show that Region 1 contains an invariant set of (2.12), i.e., an open set with the equilibrium in its interior such that the trajectories of (2.12), originating in this set, remain there (and, hence, in Region 1) for all n. To accomplish this, introduce the set $\mathscr{I}$ defined by

$$\mathscr{I} := \left\{\boldsymbol{X} : \|\boldsymbol{X} - \boldsymbol{X}_{ss}\| < 1 + \frac{1}{\sqrt{N}}\right\}, \tag{A.11}$$

where $\boldsymbol{X}_{ss} = [r, r, \ldots, r]^T$ is the steady state and $\|\cdot\|$ is the Euclidean norm of a vector.

Now, we show that $\mathscr{I} \subset$ Region 1. Since elements of $\boldsymbol{X}$ are integers, all elements of $\boldsymbol{X} \in \mathscr{I}$ are r except at most one, which is either $r+1$ or $r-1$. In other words, $\forall \boldsymbol{X} \in \mathscr{I}$, $\sum_{i=1}^{N} x_i \leqslant Nr + 1$. Moreover, based on (3.6) and taking into account that M is an integer, $Nr + 1 \leqslant M$. Therefore, $\forall \boldsymbol{X} \in \mathscr{I}$, $\sum_{i=1}^{N} x_i \leqslant M$, which implies $\mathscr{I} \subseteq$ Region 1.

Next, we show that the trajectories of (2.12) originating in $\mathscr{I}$ do not leave $\mathscr{I}$. Indeed, assume $\boldsymbol{X}(n) \in \mathscr{I}$. If one of $x_i(n)$'s, say $x_j(n)$, is $r+1$ and other elements of $\boldsymbol{X}(n)$ are r, based on FBFS or LBFS dispatch,

$$v_j(x_1(n), x_2(n), \ldots, x_N(n)) = r + 1 = x_j(n),\ v_i(x_1(n), x_2(n), \ldots, x_N(n)) = r = x_i(n),\ \forall i \neq j.$$

Similarly, when one of $x_i(n)$'s is $r-1$ and other elements of $\boldsymbol{X}(n)$ are r or when at most one of $z_{ij}(n)$'s is $r+1$ or $r-1$ and other elements of $\boldsymbol{X}(n)$ are r, we again obtain:

$$v_i(x_1(n), x_2(n), \ldots, x_N(n)) = x_i(n),\ \forall i = 1, 2, \ldots, N. \tag{A.12}$$

Substituting (A.12) in (2.12), we have:

$$\begin{aligned}
z_{01}(n+1) &= r,\\
z_{0j}(n+1) &= z_{0,j-1}(n),\ j = 2, 3, \ldots, \tau_0,\\
x_1(n+1) &= z_{0,\tau_0}(n),\\
z_{i1}(n+1) &= x_i(n),\ i = 1, 2, \ldots, N-1,\\
z_{ij}(n+1) &= z_{i,j-1}(n),\ i = 1, 2, \ldots, N-1,\ j = 2, 3, \ldots, \tau_i,\\
x_i(n+1) &= z_{i-1,\tau_{i-1}}(n),\ i = 2, 3, \ldots, N,\\
z_{N1}(n+1) &= x_N(n),\\
z_{Nj}(n+1) &= z_{N,j-1}(n),\ j = 2, 3, \ldots, \tau_N.
\end{aligned}$$

Since the vector comprising the right-hand side of these equations is in $\mathscr{I}$, the vector comprising the left-hand side is also in $\mathscr{I}$, implying that $\boldsymbol{X}(n+1) \in \mathscr{I}, \forall n \geqslant 0$. ∎

Proof of Theorem 4.3: By induction: First, we prove that states z_{0j}, $j = 1, 2, \ldots, \tau_0$, and x_1 reach their steady state value r in finite time from any finite initial condition. Indeed, no matter what $z_{0j}(0)$'s are, $z_{0j}(\tau_0) = r$, $j = 1, 2, \ldots, \tau_0$. Also, $x_1(\tau_0) \leqslant x_1(0) + \sum_{1 \leqslant j \leqslant \tau_0} z_{0j}(0)$. Therefore, since under FBFS the machines are first assigned to buffer b_1, $x_1(n) = r$, $\forall n \geqslant n_1 = \tau_0 + \left\lceil \frac{x_1(0) + \sum_{1 \leqslant j \leqslant \tau_0} z_{0j}(0)}{M - r} \right\rceil$.

Next, let state x_k, $k \in \{1, 2, \ldots, N-1\}$, reach its steady state r in finite time from any finite initial condition, i.e., $x_k(n) = r$, $\forall n \geqslant n_k$, and prove that states z_{kj}, $j = 1, 2, \ldots, \tau_k$, and x_{k+1} reach their steady state value r in finite time. For state z_{kj}, $j = 1, 2, \ldots, \tau_k$, no matter what $z_{kj}(n_k)$'s are, $z_{kj}(n_k + \tau_k) = r$, $j = 1, 2, \ldots, \tau_k$, and

$$x_{k+1}(n_k + \tau_k) \leqslant x_{k+1}(n_k) + \sum_{1 \leqslant j \leqslant \tau_k} z_{kj}(n_k) \leqslant x_{k+1}(0) + \sum_{1 \leqslant j \leqslant \tau_k} z_{kj}(0) + M n_k.$$

Therefore, under FBFS, $x_{k+1}(n) = r$, $\forall n \geqslant n_{k+1} = n_k + \tau_k + \left\lceil \frac{x_{k+1}(0) + \sum_{1 \leqslant j \leqslant \tau_k} z_{kj}(0) + M n_k}{M - (k+1) r} \right\rceil$. Note that the denominator in this expression is a positive integer because, due to $r < \frac{M}{N}$, $M - (k+1)r > (N - k - 1) r \geqslant 0$.

Finally, for state z_{Nj}, $j = 1, 2, \ldots, \tau_N$, we have $z_{Nj}(n) = r$, $\forall n \geqslant n_N + \tau_N$.

Thus, the system reaches steady state (3.5) in finite time from any finite initial condition. ∎

Proof of Lemma 4.1: First, we prove the lemma for $\tau_0 > 0$, $\tau_N = 0$ and then comment on $\tau_0 > 0$, $\tau_N > 0$.

For any finite initial condition, the system with $\tau_0 > 0$, $\tau_N = 0$ at $n = \tau_0$ reaches the state $z_{0j}(\tau_0) = r$, $j = 1, 2, \ldots, \tau_0$, and

$$\begin{aligned} &z_{i-1,j}(\tau_0) \leqslant M < \infty, \ i = 2, 3, \ldots, N, \ j = 1, 2, \ldots, \tau_{i-1}, \\ &x_i(\tau_0) \leqslant x_i(0) + \sum_{j=\max(0, \tau_{i-1} - \tau_0)}^{\tau_{i-1}} z_{i-1,j}(0) + M \max(0, \tau_0 - \tau_{i-1}) < \infty, \ i = 1, 2, \ldots, N. \end{aligned} \tag{A.13}$$

Since $\tau_0 > 0$ has no effect on machine assignment under any dispatch policy for all $n > \tau_0$, the system with $\tau_0 > 0$, $\tau_N = 0$ can be regarded as a system with $\tau_0 = 0$, $\tau_N = 0$ and initial conditions (A.13), which, due to the assumption of the lemma, is finite-time globally attractive.

In the case of $\tau_0 > 0$, $\tau_N > 0$, we observe that τ_N has no effect on machine assignment under any dispatch policy and z_{Nj}, $j = 1, 2, \ldots, \tau_N$, reach their steady states τ_N slots after x_N reached its steady state. Thus, the system with $\tau_0 > 0$, $\tau_N > 0$ is also finite-time globally attractive as long as the system $\tau_0 = 0$, $\tau_N = 0$ has this property. ■

Proof of Theorem 5.1: At the beginning of time slot $n = 1$, r lots are released to the input path of the re-entrant line. At the beginning of time slot $n = 2$, these r lots move one step in the input delay and another r lots are released. Thus, lots in the input path move forward step by step, one step in a time slot. When the first release of r lots enters into buffer b_1 at time slot $n = \tau_0 + 1$, all other buffers are still empty, which implies that, under condition (3.3), b_1 is assigned r machines according to either FBFS or LBFS dispatch. Thus, these lots are all processed and move to re-entrant path p_1. Similarly, the second release is then processed in time slot $n = \tau_0 + 2$, and then the third one and so on. In this process, each release moves forward step by step, one step in a time slot. When the first release arrives at b_2 at time slot $\tau_0 + \tau_1 + 2$, according to either FBFS or LBFS, each of b_1 and b_2 is assigned r machines, implying the situation is the same as before. Clearly, even when the first release arrives at buffer b_N, the situation is the same. In other words, each release moves forward step by step from its entering to the system to its exiting, one step in a time slot. Since a release has to move $N + \sum_{i=1}^{N} \tau_i$ steps in the system and the system arrives at the steady state when the first release completes its processing, the settling time is $N + \sum_{i=1}^{N} \tau_i$. ■

Proof of Theorem 5.2: Under the uniform allocation, all buffers are assigned $\frac{M}{N}$ and $\frac{M'}{N}$ machines before/after and during the breakdown, respectively. Thus, for the first buffer, we have the following balance equation:

$$r(T_{down} + T_{s1}^{uni}) - \frac{M'}{N} T_{down} = \frac{M}{N} T_{s1}^{uni},$$

where T_{s1}^{uni} is the duration of transient of $x_1(n)$. From this equation, we obtain:

$$T_{s1}^{uni} = \left\lceil \frac{Nr - M'}{M - Nr} T_{down} \right\rceil = \left\lceil \frac{\rho - \alpha}{1 - \rho} T_{down} \right\rceil,$$

where ρ and α are defined in (5.7).

Now, under the uniform allocation, there is no queueing in buffers b_i, $i = 2, 3, \ldots, N$, because both before/after and during the breakdown, the number of machines assigned to each buffer is identical. Therefore, the duration of transient for $x_2(n)$ is $T_{s1}^{uni} + (\tau + 1)$, for $x_3(n)$ is $T_{s1}^{uni} + 2(\tau + 1)$, and so on. Thus, the total duration of transients in the system is as given by (5.6). ■

Proof of Proposition 8.1: For equations on $PR(n)$, T_s, and T_{zeroPR}, it is easy to prove because the release r is constant and τ_0 and τ_N are delays having no effect on machine assignment to buffers. Thus, in the following, we just prove the other equations and inequalities.

For $WIP(n)$, we have

$$\begin{aligned} WIP(n; \tau_0, \tau_N) &= WIP(n; 0, \tau_N) + \tau_0 r \\ &= WIP(n; 0, 0) + \sum_{i=1}^{\tau_N} PR(n - i; 0, 0) + \tau_0 r \qquad \text{(A.14)} \\ &= WIP(n - \tau_N; 0, 0) + (\tau_0 + \tau_N) r, \ n = 1, 2, \ldots \end{aligned}$$

Then, we prove $EX_{WIP}(\tau_0, \tau_N) \leqslant EX_{WIP}(0, 0)$ and $OS_{RT}(\tau_0, \tau_N) \leqslant OS_{RT}(0, 0)$.

$$
\begin{aligned}
&\sum_{n=n_0+1}^{n_0+T_{down}+T_s(\tau_0,\tau_N)} WIP(n;\tau_0,\tau_N) - \Big(T_{down}+T_s(\tau_0,\tau_N)\Big)WIP_{ss}(\tau_0,\tau_N)\\
=&\sum_{n=n_0+1}^{n_0+T_{down}+T_s(\tau_0,\tau_N)} \Big(WIP(n-\tau_N;0,0)+(\tau_0+\tau_N)r\Big) - \Big(T_{down}+T_s(\tau_0,\tau_N)\Big)\Big(WIP_{ss}(0,0)+(\tau_0+\tau_N)r\Big)\\
=&\sum_{n=n_0+1}^{n_0+T_{down}+T_s(\tau_0,\tau_N)} WIP(n-\tau_N;0,0) - \Big(T_{down}+T_s(\tau_0,\tau_N)\Big)WIP_{ss}(0,0)\\
=&\sum_{n=n_0+1}^{n_0+T_{down}+T_s(0,0)+\tau_N} WIP(n-\tau_N;0,0) - \Big(T_{down}+T_s(0,0)+\tau_N\Big)WIP_{ss}(0,0)\\
=&\sum_{n=n_0+1}^{n_0+\tau_N} WIP(n-\tau_N;0,0) + \sum_{n=n_0+\tau_N+1}^{n_0+T_{down}+T_s(0,0)+\tau_N} WIP(n-\tau_N;0,0) - \Big(T_{down}+T_s(0,0)+\tau_N\Big)WIP_{ss}(0,0)\\
=&\tau_N WIP_{ss}(0,0) + \sum_{n=n_0+1}^{n_0+T_{down}+T_s(0,0)} WIP(n;0,0) - \Big(T_{down}+T_s(0,0)+\tau_N\Big)WIP_{ss}(0,0)\\
=&\sum_{n=n_0+1}^{n_0+T_{down}+T_s(0,0)} WIP(n;0,0) - \Big(T_{down}+T_s(0,0)\Big)WIP_{ss}(0,0)
\end{aligned}
$$

Thus, we have

$$
\begin{aligned}
EX_{WIP}(\tau_0,\tau_N) =& \frac{\sum_{n=n_0+1}^{n_0+T_{down}+T_s(\tau_0,\tau_N)} WIP(n;\tau_0,\tau_N) - \Big(T_{down}+T_s(\tau_0,\tau_N)\Big)WIP_{ss}(\tau_0,\tau_N)}{\Big(T_{down}+T_s(\tau_0,\tau_N)\Big)WIP_{ss}(\tau_0,\tau_N)}\\
=&\frac{\sum_{n=n_0+1}^{n_0+T_{down}+T_s(0,0)} WIP(n;0,0) - \Big(T_{down}+T_s(0,0)\Big)WIP_{ss}(0,0)}{\Big(T_{down}+T_s(0,0)+\tau_N\Big)\Big(WIP_{ss}(0,0)+(\tau_0+\tau_N)r\Big)}\\
\leqslant&\frac{\sum_{n=n_0+1}^{n_0+T_{down}+T_s(0,0)} WIP(n;0,0) - \Big(T_{down}+T_s(0,0)\Big)WIP_{ss}(0,0)}{\Big(T_{down}+T_s(0,0)\Big)WIP_{ss}(0,0)}\\
=&EX_{WIP}(0,0).
\end{aligned}
$$

For OS_{RT},

$$
\begin{aligned}
OS_{RT}(\tau_0,\tau_N) =& \frac{RT_{\max}(T_{down};\tau_0,\tau_N) - RT_{ss}(\tau_0,\tau_N)}{RT_{ss}(\tau_0,\tau_N)} \\
=& \frac{\Big(RT_{\max}(T_{down};0,0) + (\tau_0+\tau_N)r\Big) - \Big(RT_{ss}(0,0) + (\tau_0+\tau_N)r\Big)}{RT_{ss}(0,0) + (\tau_0+\tau_N)r} \\
\leqslant& \frac{RT_{\max}(T_{down};0,0) - RT_{ss}(0,0)}{RT_{ss}(0,0)} \\
=& OS_{RT}(0,0).
\end{aligned}
$$

Finally, we prove the last two equations. Based on the definition of variability of WIP, we have

$$
V(WIP;\tau_0,\tau_N) = \sum_{n=n_0+1}^{n_0+T_{down}+T_s(\tau_0,\tau_N)} \left| WIP(n;\tau_0,\tau_N) - WIP(n-1;\tau_0,\tau_N) \right|.
$$

Substituting (A.14) in the above equation, we obtain

$$
\begin{aligned}
V(WIP;\tau_0,\tau_N) =& \sum_{n=n_0+1}^{n_0+T_{down}+T_s(0,0)+\tau_N} \left| WIP(n-\tau_N;0,0) - WIP(n-\tau_N-1;0,0) \right| \\
=& \sum_{n=n_0+1}^{n_0+\tau_N} \left| WIP(n-\tau_N;0,0) - WIP(n-\tau_N-1;0,0) \right| + \\
& \sum_{n=n_0+\tau_N+1}^{n_0+T_{down}+T_s(0,0)+\tau_N} \left| WIP(n-\tau_N;0,0) - WIP(n-\tau_N-1;0,0) \right| \\
=& \sum_{n=n_0+\tau_N+1}^{n_0+T_{down}+T_s(0,0)+\tau_N} \left| WIP(n-\tau_N;0,0) - WIP(n-\tau_N-1;0,0) \right| \\
=& \sum_{n=n_0+1}^{n_0+T_{down}+T_s(0,0)} \left| WIP(n;0,0) - WIP(n-1;0,0) \right| \\
=& V(WIP;0,0).
\end{aligned}
$$

Similarly, for $V(PR)$,

$$
\begin{aligned}
V(PR;\tau_0,\tau_N) &= \sum_{n=n_0+1}^{n_0+T_{down}+T_s(\tau_0,\tau_N)} |PR(n;\tau_0,\tau_N) - PR(n-1;\tau_0,\tau_N)| \\
&= \sum_{n=n_0+1}^{n_0+T_{down}+T_s(0,0)+\tau_N} |PR(n-\tau_N;0,0) - PR(n-\tau_N-1;0,0)| \\
&= \sum_{n=n_0+1}^{n_0+\tau_N} |PR(n-\tau_N;0,0) - PR(n-\tau_N-1;0,0)| + \\
&\quad \sum_{n=n_0+\tau_N+1}^{n_0+T_{down}+T_s(0,0)+\tau_N} |PR(n-\tau_N;0,0) - PR(n-\tau_N-1;0,0)| \\
&= \sum_{n=n_0+\tau_N+1}^{n_0+T_{down}+T_s(0,0)+\tau_N} |PR(n-\tau_N;0,0) - PR(n-\tau_N-1;0,0)| \\
&= \sum_{n=n_0+1}^{n_0+T_{down}+T_s(0,0)} |PR(n;0,0) - PR(n-1;0,0)|
\end{aligned}
$$

■

References

[1] R. G. Askin and C. R. Standridge, *Modeling and Analysis of Manufacturing Systems*. New York: Wiley, 1993.

[2] J. A. Buzacott and J. G. Shanthikumar, *Stochastic Models of Manufacturing Systems*. Englewood Cliffs, N.J.: Prentice Hall, 1993.

[3] H. T. Papadopoulos, C. Heavey, and J. Browne, *Queueing Theory in Manufacturing Systems Analysis and Design*. London: Chapman & Hall, 1993.

[4] S. B. Gershwin, *Manufacturing Systems Engineering*. Englewood Cliffs, N.J.: PTR Prentice Hall, 1994.

[5] J. Li and S. M. Meerkov, *Production Systems Engineering*. New York: Springer, 2009.

[6] O. Rose, "WIP evolution of a semiconductor factory after a bottleneck workcenter breakdown," in *Proceedings of the 1998 Winter Simulation Conference*, 1998, pp. 997–1003.

[7] ——, "Estimation of the cycle time distribution of a wafer fab by a simple simulation model," in *Proceedings of the International Conference on Semiconductor Manufacturing Operational Modeling and Simulation*, 1999, pp. 133–138.

[8] ——, "Why do simple wafer fab models fail in certain scenarios," in *Proceedings of the 2000 Winter Simulation Conference*, 2000, pp. 1481–1490.

[9] ——, "Improving the accuracy of simple simulation models for complex production systems," in *Proceedings of the 2007 INFORMS Simulation Society Research Workshop*, 2007.

[10] T. Beaumariage and K. Kempf, "The nature and origin of chaos in manufacturing systems," in *IEEE/SEMI Advanced Semiconductor Manufacturing Conference*, 1994, pp. 169–174.

[11] D. Armbruster, D. E. Marthaler, C. Ringhofer, K. Kempf, and T.-C. Jo, "A continuum model for a re-entrant factory," *Operations Research*, vol. 54, no. 5, pp. 933–950, 2006.

[12] P. R. Kumar, "Re-entrant lines," *Queueing Systems*, vol. 13, no. 1-3, pp. 87–110, 1993.

[13] L. M. Wein, "Scheduling semiconductor wafer fabrication," *IEEE Transactions on Semiconductor Manufacturing*, vol. 1, no. 3, pp. 115–130, 1988.

[14] J. W. Fowler, S. Brown, H. Gold, and Schömig, "Measurable improvements in cycle-time-constrained capacity," in *Proceedings of the 6th International Symposium on Semiconductor Manufacturing*, 1997, pp. A21– A24.

[15] R. T. Johnson, J. W. Fowler, and G. T. Mackulak, "A discrete event simulation model simplification technique," in *Proceedings of the 2005 Winter Simulation Conference*, 2005, pp. 2172–2176.

[16] I. A. El-Khouli, K. S. El-Kilany, and A. E. El-Sayed, "Modeling and simulation of re-entrant flow shop scheduling: An application in semiconductor manufacturing," in *2009 International Conference on Computers and Industrial Engineering*, 2009, pp. 211–216.

[17] S. Kim, J. F. Cox, and V. J. Mabin, “An exploratory study of protective inventory in a re-entrant line with protective capacity,” *International Journal of Production Research*, vol. 48, no. 14, pp. 4153–4178, 2010.

[18] Z. G. Jiang, M. Dong, P. Tian, and D. Yang, “Modeling and simulation of re-entrant lines semiconductor wafer fabrication lines with PM using GSPN,” *Advanced Materials Research*, vol. 97-101, pp. 2469–2472, 2010.

[19] J. G. Dai and G. Weiss, “Stability and instability of fluid models for re-entrant lines,” *Mathematics of Operations Research*, vol. 21, no. 1, pp. 115–134, 1996.

[20] Y. Guo, J. Yang, and X. Wang, “Stability of a 2-station-5-class re-entrant line with infinite supply of work,” *Asia-Pacific Journal of Operations research*, vol. 25, no. 4, pp. 477–493, 2008.

[21] Y. Guo, “Fluid model criterion for instability of re-entrant line with infinite supply of work,” *TOP*, vol. 17, no. 2, pp. 305–319, 2009.

[22] I. M. MacPhee and L. J. Mueller, “Stability criteria for multi-class queuing networks with re-entrant lines,” *Methodology and Computing in Applied Probability*, vol. 9, no. 3, pp. 377–388, 2007.

[23] M. K. Omar, S. Kumar, and Y. Suppiah, “Performance analysis in a re-entrant operation with combinational routing and yield probabilities,” *Applied Mathematical Modeling*, vol. 33, no. 3, pp. 1601–1612, 2009.

[24] C. Wang and J. Li, “Approximate analysis of re-entrant lines with Bernoulli reliability models,” *IEEE Transactions on Automation Science and Engineering*, vol. 7, no. 3, pp. 708–715, 2010.

[25] W. Rudin, *Real and Complex Analysis*. New York: McGraw-Hill, 2006.

[26] F. Brauer and J. A. Nohel, *The Qualitative Theory of Ordinary Differential Equations: An Introduction*. New York: Dover, 1989.

[27] J. Guckenheimer and P. Holmes, *Nonlinear Oscillations, Dynamical Systems, and Bifurcations of Vector Fields*. New York: Springer-Verlag, 1983.

[28] C. Glassey, J. Shanthikumar, and S. Seshadri, "Linear control rules for production control of semiconductors fabs," *IEEE Transactions on Semiconductor Manufacturing*, vol. 9, no. 4, pp. 536–549, 1996.

[29] J. W. Fowler, G. L. Hogg, and S. J. Mason, "Workload control in the semiconductor industry," *Production Planning and Control*, vol. 13, no. 7, pp. 568–578, 2002.

[30] R. M. Dabbas and J. W. Fowler, "A new scheduling approach using combined dispatching criteria in wafer fabs," *IEEE Transactions on Semiconductor Manufacturing*, vol. 16, no. 3, pp. 501–510, 2003.

[31] F. D. Vargas-Villamil, D. E. Rivera, and K. G. Kempf, "A hierarchical approach to production control of re-entrant semiconductor manufacturing lines," *IEEE Transactions on Control Systems Technology*, vol. 11, no. 4, pp. 578–587, 2003.

[32] A. Zafra-Cabeza, M. A. Riado, E. F. Camacho, K. G. Kempf, and D. E. Rivera, "Managing risk in semiconductor manufacturing: A stochastic predictive control approach," *Control Engineering Practice*, vol. 15, no. 8, pp. 969–984, 2007.

[33] Z. Wang, Q. Wu, and F. Qiao, "A lot dispatching strategy integrating WIP management and wafer start control," *IEEE Transactions on Automation Science and Engineering*, vol. 4, no. 4, pp. 579–583, 2007.

[34] D. Perdaen, D. Armbruster, K. Kempf, and E. Lefeber, "Controlling a re-entrant manufacturing line via the push-pull point," *International Journal of Production Research*, vol. 46, no. 16, pp. 4521–4536, 2008.